High-Efficiency SiC Power Conversion – Base Drivers for Bipolar Junction Transistors and Performance Impacts on Series-Resonant Converters

GEORG TOLSTOY

Doctoral Thesis
Stockholm, Sweden 2015

Electrical Energy Conversion
School of Electrical Engineering
KTH Royal Institute of Technology
Teknikringen 33
SE-100 44 Stockholm
SWEDEN

TRITA-EE 2015:024
ISSN 1653-5146
ISBN 978-91-7595-601-5

Akademisk avhandling som med tillstånd av Kungl Tekniska högskolan framlägges till offentlig granskning för avläggande av teknologie doktorsexamen fredagen den 12:e juni 2015 klockan 10.15 i Sal H1, Kungl Tekniska högskolan, Teknikringen 33, Stockholm.

© Georg Tolstoy, Maj 2015

Tryck: Universitetsservice US AB

till min familj

Sammanfattning

Denna avhandlings syfte är att skapa en förståelse för kiselkarbid (SiC) teknologin. SiC-transistorer är vida överlägsna insulated-gate bipolar transistorer (IGBTer) i kisel på flera sätt. De är effektivare, kan arbeta vid högre switchfrekvenser samt kan användas vid högre temperaturer. Om SiC-transistorer används i en effektomvandlare skulle behovet av kylning minskas, vilket i sin tur minskar kostnaden och komplexiteten för kylsystemet. En annan fördel är att omvandlaren kan göras lättare och mindre då man kan arbeta vid högre switchfrekvenser.

De tre huvudsakliga SiC-transistorerna, bipolar junction transistor (BJT), junction field-effect transistor (JFET) och metal-oxide semiconductor field-effect transistor (MOSFET), diskuteras med fokus på BJT. Potentialen för att applicera SiC-transistorer i produkter diskuteras. SiC-teknologin har potential inom många områden, från induktionsvärmning till högspänd likströmstransmission.

Olika koncept för basdrivdon presenteras och drivdonseffektförbrukningen härleds. Vidare presenteras det första proportionella drivdonet för SiC BJTer. Detta drivdon bygger på diskreta basströmsnivåer. Det introducerade drivdonet konstrueras och testas i en prototyp. Beroende på lastströmmen kan drivdonseffektförbrukningen reduceras markant.

I denna avhandling presenteras också den första diskussionen om backledning i en SiC-BJT. Det visar sig viktigt att ha detta i åtanke då designen av basdrivdonet görs.

Sist undersöks effekterna av att använda sig av SiC-MOSFETar och SiC-BJTer i en serieresonans (SLR) omvandlare. Två H-bryggor har undersökts, en med SiC-MOSFETar som använder sig av bodydioden för backledning under dödtiden, och den andra med SiC-BJTer med antiparallella Schottkydioder. SiC-transistorer är ideala för att använda i applikationer där mjuka till- och frånslag används då de saknar tail-strömmar. SiC-MOSFETar drar även nytta av att kunna leda strömmen under backledningstiden då detta ger ett lägre spänningsfall än om strömmen skulle gå i bodydioden. Det har också visat sig att storleken på kapacitansen hos snubbers kan reduceras jämfört med dagens kiselteknologi. Höga switchfrekvenser på 200 kHz kan uppnås, samtidigt som förlusterna hålls låga.

Denna avhandling visar också på vikten av korrekt styrning. Att optimera längden för dödtiden visar sig vara viktigt för att reducera förlusterna. Dual control (DuC) testas också i kombination med SiC-transistorerna. Jämfört med frekvensmodulering (FM) uppnås lägre förluster med MOSFET-bryggan.

Alla analytiska undersökningar som läggs fram i denna avhandling är bekräftade genom experiment.

Nyckelord: Kiselkarbid (SiC), bipolär transistor (BJT), resonant omvandlare, serieresonant omvandlare (SLR), basströmsdrivdon, högeffekta omvandlare, högfrekventa omvandlare.

Abstract

This thesis aims to bring an understanding to the silicon carbide (SiC) bipolar junction transistor (BJT). SiC power devices are superior to the silicon IGBT in several ways. They are for instance, able to operate with higher efficiency, at higher frequencies, and at higher junction temperatures. From a system point of view the SiC power device could decrease the cost and complexity of cooling, reduce the size and weight of the system, and enable the system to endure harsher environments.

The three main SiC power device designs are discussed with a focus on the BJT. The SiC BJT is compared to the SiC junction field-effect transistor (JFET) and the metal-oxide semiconductor field-effect transistor (MOSFET). The potential of employing SiC power devices in applications, ranging from induction heating to high-voltage direct current (HVDC), is presented.

The theory behind the state-of-the-art dual-source (2SRC) base driver that was presented by Rabkowski et al. a few years ago is described. This concept of proportional base drivers is introduced with a focus on the discretized proportional base drivers (DPBD). By implementing the DPBD concept and building a prototype it is shown that the steady-state consumption of the base driver can be reduced considerably.

The aspects of the reverse conduction of the SiC BJT are presented. It is shown to be of importance to consider the reduced voltage drop over the base-emitter junction.

Last the impact of SiC unipolar and bipolar devices in series-resonant (SLR) converters is presented. Two full-bridges are designed and constructed, one with SiC MOSFETs utilizing the body diode for reverse conduction during the dead-time, and the second with SiC BJTs with anti-parallel SiC Schottky diodes. It is found that the SiC power devices, with their absence of tail current, are ideal devices to fully utilize the soft-switching properties that the SLR converters offer. The SiC MOSFET benefits from its possibility to utilize reverse conduction with a low voltage drop. It is also found that the size of capacitance of the snubbers can be reduced compare to state-of-the-art silicon technology. High switching frequencies of 200 kHz are possible while still keeping the losses low. A dead-time control strategy for each device is presented. The dual control (DuC) algorithm is tested with the SiC devices and compared to frequency modulation (FM).

The analytical investigations presented in this thesis are confirmed by experimental results on several laboratory prototype converters.

Keywords: Silicon Carbide, Bipolar Junction Transistor (BJT), Resonant converter, Series-resonant converter (SLR), Base drive circuits, High-Efficiency Converters, High-Frequency Converters.

Acknowledgements

This thesis concludes the work that I have carried out at the Laboratory of Electrical Energy Conversion, KTH Royal Institute of Technology since January 2009. Even though the work of the Ph.D. student is solitary, this thesis would never have happened without the guidance and encouragement of certain people.

First of all, I would like to express great gratitude to my supervisor Professor Hans-Peter Nee. Especially for his guidance during these years. *Hansi* has been a great supervisor and his knowledge in power electronics is second to none

I would also like to show my gratitude towards Professor Jacek Rabkowski from Warsaw Institute of Technology. He was a great mentor during his stay at our lab. He assisted in the early parts of my research, especially with the practical parts, with building prototypes and collecting valuable data.

Dr. Per Ranstad was a large part of the last part of my thesis. He has have provided me with technical knowledge and guidance, as well as continuous encouragement throughout the project. I hope we can continue our scientific discussions in the future. I would also like to thank Florian Gitzendanner and R. Al Sundook for assisting me during my time in Växjö.

I would like to acknowledge my namesake, Dr. Georgios Demitriades, from ABB CRC. Even do he has not contributed directly to this thesis he is one the reasons I am where I am today. He found me in ABB's master thesis database (Query: 'Georg*') and brought me to ABB in Västerås to do my Master Thesis. He then approached me some year later, when I was working as a software developer, to see if I should apply for a Ph. D position at E2C, KTH. Which I did.

Special thanks also goes to my device specialists in Kista. To my co-supervisor Dr. Mietek Bakowski who knows what there is to know about device physics, and can always answer a question. To my collegue and soon-to-be-Dr Jang-Kwon Lim who have helped assisted me in many things.

Thanks also to my part-time supervisor at Cambridge University, Dr. Patrick Palmer who co-author a publication with me. I would also like to thank the Cambrisge University Ice Hockey Club for having me on your team during the two years I spent in Cambridge.

Many thanks to all my colleagues at KTH for making the workplace more than enjoyable. First I would like to thank past and present members of the SiC group: Dimosthenis Peftitsis, Juan Colmenares, and Diane Sadik. I have always felt your friendship and it has been easy discussing all matter of things. I never felt stupid asking the dumbest questions, but they usually turned into interesting discussions that would move our work forward. I have learned a lot in the lab and office with you, and you are a big part of this thesis. I would also like to thank Eva Pettersson for not just being our economist but also a good friend. This is also extended to our vital staff, Peter Lönn, Jesper Friberg, and Alija Cosic. I will also remember Olle Brännvall who is no longer with us. There have been many people in the lab during the time I have been here. Some I would like to mention are Antonious, Kalle, Tomas, Luca, Naveed, Andreas, Alex, Erik, Noman, Emma, Celie but also the rest of you have been great company at KTH but also abroad on conferences. Also thanks to the innebandy team at EES. My former project worker Björn Larsson will get a special mentioning. The work we carried out together could not fit in the scope of this thesis. Even though I supervised him, we became friends and he succeed with his studies to go work for ABB traction.

The last three years of my thesis I have spent on traveling foot from my family in Karlskoga. This has been hard, not just for me, but for people around me. I would like to thank my parents, Gunnel and Nikolaj, for being there and encouraging me onwards and helping me out in different ways. Without the two of you this thesis would never have been finalized. I am also grateful to my brother Tedde and his family, Stina, Ester, and Viktor and to my friend Joi Widstrand and his family, Elinor, Filip, and Nea, these families have invited me for dinner every week and taken care of me. I would also like to mention my friends who have made my stay in Stockholm feel less lonely by encouraging my company and activities with me. Thank you Niklas, Ville, Maria, Alek, Josefin, Axel, Jessica, Linn, Jacob, kusin Johan, Lena and David.

Last, but absolutely not least, I would like to thank my family. My dear Dora and Edgar, who have never lived a day in their life without a Ph.D student of a father. I have been away much, but I have also tried to be more present when home. I hope you have not been scarred for life, but instead will understand the joy of learning. And to my wife Päivi who has encouraged me and shown great patience with me. These years have been the best and worst for us in many ways. I love you and promise you that this will be the last Ph.D. thesis I write.

Stockholm, May 2015
Georg Tolstoy

“Jag har väntat så länge på just den här dan
Och det är skönt att den äntligen kommer
Väntat så länge på just den här dan
Den ger lust, när den kommer”

— Aapo Sääsk*, 1979*

Contents

Contents **xiii**

1 Introduction **1**
1.1 Background . . . 1
1.2 Main objectives . . . 3
1.3 Methodology . . . 4
1.4 Main Contributions . . . 4
1.5 Outline of the Thesis . . . 5
1.6 List of Appended Publications . . . 5
1.7 Related Publications . . . 8

2 SiC Power Devices and Applications **11**
2.1 SiC Power Devices . . . 13
2.2 Why Silicon Carbide Bipolar Junction Transistors? . . . 16
2.3 Applications for SiC power devices . . . 18

3 Base Drivers for Silicon Carbide Bipolar Junction Transistors **23**
3.1 Introduction to Base Drivers . . . 23
3.2 Base Drive Concepts . . . 24
3.3 Proportional Base Driver Concepts . . . 29
3.4 Reverse Conduction of SiC BJTs and the Relation to Base Drivers . 35

4 SiC unipolar and bipolar power devices in a SLR converter **39**
4.1 Basics of the SLR Converter with Capacitive Snubbers . . . 40
4.2 Analysis of Losses in the Full-Bridge . . . 41
4.3 Experimental setup . . . 45
4.4 Discussion of results . . . 50

5 Conclusions and Future Work **59**
5.1 Conclusions . . . 59

5.2 Future Work 60

List of Acronyms **63**

Bibliography **65**

Publication I **73**

Publication II **75**

Publication III **77**

Publication IV **79**

Publication V **81**

Publication VI **83**

Publication VII **85**

Publication VIII **87**

Chapter 1

Introduction

1.1 Background

From the first law of thermodynamics it is understood that energy can never be created or destroyed, but it is possible to change the form of the energy and to transfer it. One of these forms is electricity. It is easy to transform many kinds of energy sources into electric energy. Electric energy is also easy to transfer and to use. In some applications, i.e. mobile phone batteries, it is also possible to store a sufficient amount of energy. Electricity itself can have many forms, direct current (dc) or alternating current (ac) of different frequencies and forms, high voltage or low voltage, and so on. To be able to use the 230 V/50 Hz *ac* plug in your home to charge your 5 V *dc* mobile phone or to use your 100 kHz *ac* high-frequency induction-stove, power electronics is necessary. The form of the electricity is transformed many times by power electronics as the energy from the sun is transformed into electricity and heat in a PV-panel, until it becomes heat in your meatballs and spaghetti on your induction stove.

Today, the purpose of power electronics research is twofold: finding new applications and improving already existing power electronic applications. New applications in history are for example, when the train got electrified (Robert Davidson, 1837 [1]), wind turbines(James Blyth, 1887 [2]), voltage-source-converter-based high-voltage dc (HVDC) transmission (Hällsjön Link) [3]), etc. But what is more common is that the invention gets upgraded. The charger gets smaller, the electric vehicle (EV) is able to drive further, the fridge consumes less energy, etc. When these upgrades occur, it is usually because the new product is smaller, lighter, hotter, cooler, more energy efficient, or as usually happens, a combination of these [4]. Many of these upgrades are made possible whenever a new era in power electronic switches is initiated [5]. From the mercury arc valve era [6], to the power bipolar

junction transistor (BJT) era (60's-90's) [7, 8], to the metal-oxide semiconductor field-effect transistor (MOSFET) era (70's-today) [9], and to the insulated-gate bipolar transistor (IGBT) era (90's-today) [10, 11] the improvement of power semiconductors has made the improvement of products and our society possible.

The drive for new devices today does not just originate from an economical standpoint, but also from an environmental one. As the world gets ever more electrified, every small gain in efficiency means a lot, both in saved dollars as well as reduced CO_2 emissions. This drive, to improve from today's silicon (Si) devices, has shifted the focus towards new materials that have improved properties. These materials are called wide band gap (WBG) materials, including for instance, gallium nitride (GaN) [12], and silicon carbide (SiC) [5]. Some of the material properties can be seen in Table 1.1.

These properties enable SiC and GaN devices to have higher voltage ratings, lower voltage drops, higher maximum temperatures, and higher thermal conductivities, bringing the SiC devices closer to the ideal switch than the silicon devices.

In the early 90's a great push to manufacture SiC power devices was made [13]. In 1999 ABB was ready to launch its first component, but it was delayed [14]. Two years later they canceled their $ 50 M, 8 year project, due to the imperfections in the SiC wafers [15]. The material development of SiC continued and prospered, mainly due to SiC having an important role in today's led-light revolution. Today the material is grown with very few defects on six inch wafers [16]. Eight inch wafers are starting to be introduced. As the size of the wafers grows, the prize of substrates for SiC device manufacturing goes down.

The hope of the WBG industry is that GaN switches, which were introduced to the market last year, will take a dominant part in power electronic applications below 600 V. The SiC switches, which have been on the market for some years, target devices with blocking voltages of 1.2 kV and upwards. It is believed that unipolar SiC devices, such as the junction field effect transistor (JFET) and MOSFET, will be competitive up to 4.5 kV where the bipolar devices, BJT and IGBT, will have a larger impact [17, 18]. On the market today, GaN devices up to 600 V can be purchased. SiC devices on the market today range from 600 V up to 1700 V. It should be noted that SiC Schottky diodes, [19], have been on the market since the

Table 1.1: Physical properties of Silicon, Silicon Carbide and Gallium Nitride.

Properties	**Material**	**Si**	**4H-SiC**	**GaN**
E_g [eV]	bandgap	1.1	3.3 V	3.4 V
λ [W/cm· K]	thermal conductivity	1.5	4.5	1.3
E_g [10^6 V/cm]	breakdown voltage	0.3	2.4	3.3

early years of the millennium, and have improved the turn-ON efficiency of the Si IGBT due to its (almost) non-existing reverse recovery.

What is holding back the industry from throwing out their Si devices and replacing them with the improved WBG devices are three issues:

1. Reliability - The history of the failures in the early years of the millennium [15] is fresh in mind, and nobody wants to be first with a large scale upgrade without the new technology being thoroughly tested. However, change is coming. Two vehicle manufacturers are currently testing SiC power electronics in new products.

2. Packaging - To fully be able to utilize the SiC devices, packaging has to improve [20]. The improvement should focus on reducing the parasitic inductance and making the module withstand higher temperatures than today's 175 °C which is the maximum temperature for silicon. Also, power cycling may become an issue for the SiC device packaging because with higher maximum temperature it is also likely that the temperature cycles will have a higher amplitude. The power module makers have identified these problems and may move away from bond-wires to other solutions of connecting the terminals.

3. Fear of change - As always, new technologies are met with skepticism. The hope is that this thesis will shed some light on how efficient the SiC technology is and how easy it is to adapt to the new WBG technology.

When this project started the joke in SiC industry was that it was always 5 years from a large breakthrough. This was said in 2009, and had been said every year in the preceding 10 year period. However, it is the opinion of the author that 2015 is the year of breakthrough for SiC switches. It is also the hope of the author that the research this thesis builds upon has been a small part of the big puzzle that has taken us into the WBG era.

1.2 Main objectives

The main objectives of work presented in this thesis are:

- Propose efficient base drivers for SiC power BJTs.
- Demonstrate successful examples of power converters with SiC power devices.
- Create an understanding of how the efficiency can be increased by introducing SiC power switches in resonant converters.

- Create an understanding of how the total system cost can be reduced by introducing SiC power switches.

1.3 Methodology

The findings in this thesis are mainly derived from theoretical analyses that have been proven by simulations and experiments. The experimental validations have been carried out by measuring the voltage and current waveforms by means of voltage probes and Rogovski-coils for the current measurement. The loss measurements have been carried out by means of electrical, thermo-electrical or calorimetric measurements.

1.4 Main Contributions

This thesis is divided into three different parts.

The main contribution of the first part is a study of how the low ON-state resistance of the normally-ON SiC JFET could impact a 300 MW modular multilevel converter with regard to losses. This is one of the most promising future applications of SiC power electronics. This investigation was a teamwork with several persons involved. The author of this thesis was, however, one of the most important contributors, especially regarding the experimental verification, loss calculations, and final preparation of the manuscript.

The main contribution of the second part is towards base drivers for SiC power BJTs. Two driver concepts have been proposed, designed and tested. The first one, introduced by Rabkowski et al., is the *2SRC base driver* which showed that it is possible to have fast switching transients without increasing the steady-state consumption of the base driver. The author of this thesis took part in a team work where the author assisted the main contributor Jacek Rabkowski.

The second base driver concept is the *discretized proportional base driver*, which can reduce the steady-state losses even further. This is done by reducing the base-current when a lower collector current flows through the device. This is the first time a proportional base driver concept for SiC BJTs is presented. It is shown that the base current can be limited without increasing the ON-state voltage-drop. In this work, the author of this thesis was the main contributor.

In the third part, the author's research was dedicated to investigating the impact of SiC power switches on the performance of series-resonant converters. The first main contribution is a theoretical and experimental investigation on how the dead-time control of the SiC unipolar and bipolar devices impacts the losses. The novelty lies in the proposed dead-time control as well as the discussion about the aspects of

SiC BJT reverse conduction. In this work, the author of this thesis was the main contributor.

Other contributions are the experimental verification on how well the dual control algorithm works with SiC devices in series-resonant converters as well as an investigation on how the size of the capacitive snubber and the switching frequency impacts the losses. In this work, the author of this thesis was the main contributor.

1.5 Outline of the Thesis

Chapter 2 presents SiC devices and their applications, and also gives a deeper view of the SiC power BJT.

Chapter 3 describes the concepts of base drivers for SiC power BJTs, and discusses the reverse conduction of SiC BJTs.

Chapter 4 presents the impact that SiC power devices can have on series-resonant converters.

Chapter 5 summarizes the work presented in this thesis and gives ideas and suggestions for future research in this field.

1.6 List of Appended Publications

I. **G. Tolstoy**, D. Peftitsis, J. Rabkowski and H.–P. Nee, "Performance tests of $4.1x4.1mm^2$ SiC JFETs for a DC/DC boost converter application", *in Proc. of* 8^{th} *European Conference on Silicon Carbide and Related Materials 2010*, ECSCRM 2010, pp. 722–725, 29 Aug.–2 Sept. 2010.

This is the first characterization of the $4.1x4.1mm^2$ SiC LCVJFET from SiCED. The static characterization shows a positive temperature coefficient of the ON-state resistance as well as a small negative temperature coefficient of the voltage across the intrinsic body diode.

The main contribution by the author to this publication was to do the static characterization of the device as well as the short circuit test, and to prepare the manuscript.

II. D. Peftitsis, **G. Tolstoy**, A. Antonopoulos, J. Rabkowski, J.–K. Lim, M. Bakowski, L. Ängquist, and H.–P. Nee, "High-power modular multilevel converters with SiC JFETs", *IEEE Trans. Power Electron.*, vol. 27, no. 1, pp.

28–36, Jan. 2012.

This paper studies the possibility of using SiC unipolar power switches in a modular multilevel converter (M2C). The idea is to compare the low ON-state resistance of the SiC JFET and SiC BJT with state-of-the-art silicon devices of today. Experimental results show the feasibility of using SiC normally-ON JFETs in such a converter. Furthermore, the power losses of a future SiC M2C have been theoretically estimated using simulations from two high-voltage normally-ON SiC JFETs.

The main contribution by the author to this publication was the design and layout of the submodule populated with SiC JFETs instead of Si MOSFETs which is the most vital part to experimentally verify the ideas presented in **Publication II**. The author validated the functions of the SiC JFET submodule before installing it in the M2C converter, and then assisted with the experimental procedure. The author also contributed by performing most of the final efficiency calculations and preparing parts of the manuscript, especially the part discussing the possibility to use SiC BJTs in the M2C.

III. J. Rabkowski, **G. Tolstoy**, D. Peftitsis and H.–P. Nee, "Low-loss high-performance base-drive unit for SiC BJTs", *IEEE Trans. Power Electron.*, vol. 27, no. 5, pp. 2633–2643, May 2012.

Publication III is a solution for an energy efficient and fast switching base driver for SiC power BJTs. Different parts of the power consumption are identified and verified by experiments. The proposed driver is tested in a boost converter obtaining switching speeds well below 50 ns. This is the first base driver for SiC BJTs in literature that provides a solution for low steady-state power consumption while switching with fast transients.

The main contribution by the author to this publication was to assist with the experimental procedure, to assist with the loss and efficiency calculations for the manuscript, and to substantially contribute in finalizing the writing of the manuscript. Jacek Rabkowski performed most of the work, with the author of this thesis and Dimosthenis Peftitsis assisting him.

IV. **G. Tolstoy**, D. Peftitsis, J. Rabkowski, P. R. Palmer, and H.–P. Nee, "A discretized proportional base driver for silicon carbide bipolar junction transistors", in *IEEE Transactions on Power Electronics*, vol. 29, no. 5, pp.

2408–2417, May 2014.

Publication IV is the first publications that discusses the possibility of a proportional base driver for SiC power BJTs. This publication builds upon the theory of **Publication III** and shows how it is possible to reduce the steady-state power consumption of the base driver even further. A discretized proportional base driver is proposed, constructed and tested in a boost converter. Finally, a loss analysis is conducted to see how much the base driver power consumption can be reduced for an application in an electrical vehicle driving the *New European Drive Cycle*.

The author did almost all of the work in this publication. The contributions to this publications was to identify the concept of proportional drivers for SiC BJT, designing and building the DPBD prototype, making a experimental setup, conducting the tests, loss and efficiency calculations, and preparation of the manuscript.

V. **G. Tolstoy**, P. Ranstad, J. Colmenares, D. Peftitsis, F. Giezendanner, J. Rabkowski, and H.–P. Nee, "An experimental analysis on how the dead-time of SiC BJT and SiC MOSFET impacts the losses in a high-frequency resonant converter", *in Proc. of* 16^{th} *European Conference on Power Electronics and Applications (EPE 2014)*, 26–28 Aug. 2014.

VI. **G. Tolstoy**, P. Ranstad, J. Colmenares, D. Peftitsis, F. Giezendanner, J. Rabkowski, and H.–P. Nee, "An experimental analysis on how the dead-time of SiC BJT and SiC MOSFET impacts the losses in a high-frequency resonant converter", *Submitted for review in IEEE Transactions on Power Electronics.*

Publication V and the extended version, **Publication VI**, investigate how the choice of the dead-time control algorithm in a series-resonant converter, utilizing unipolar or bipolar SiC devices, impacts the losses of the full-bridge. It is shown that the control methods for the two devices are different. The theory is proven by experiments. Finally, an analysis is performed of what occurs during reverse conduction of the BJT and its relation to the base driver. Both publications are included since the extended version only has been submitted while the conference paper has been previously presented at IEEE ECCE Asia 2014.

The main contributions to these publications were to identify the control methods for unipolar and bipolar devices in resonant converters, performing

a major part of the design and construction of the experimental setup, performing all experiments, loss and efficiency calculations and preparations of the manuscripts.

VII. **G. Tolstoy**, P. Ranstad, J. Colmenares, F. Giezendanner, and H.–P. Nee, "Dual control used in series-loaded resonant converter with SiC devices", *Accepted for publication in the* 9th *IEEE International Conference on Power Electronics–ECCE Asia (ICPE ECCE)*, Jun. 2015

Publication VII investigates the potential efficiency gains that can be achieved by using dual control in combination with SiC power switches. It is shown that the unipolar SiC MOSFET shows greater potential than the bipolar SiC BJT. This is due to the possibility of the MOSFET to conduct the current in the reverse direction.

The main contributions to this publication were to perform a major part of the designing and building of the experimental setup, performing all experiments, loss and efficiency calculations and preparation of the manuscript.

VIII. **G. Tolstoy**, P. Ranstad, J. Colmenares, F. Giezendanner, and H.–P. Nee, "Experimental evaluation of SiC BJT and SiC MOSFET in a series resonant converter", *Accepted for publication in the* 17th *European Conference on Power Electronics and Applications (EPE 2015)*, Sep. 2015

SiC unipolar and bipolar devices in a series-resonant converter are investigated in Publication VIII. The focus lies on investigating how the losses are impacted by: resonant tank frequency, size of snubber capacitance, and by the choice of SiC power device, BJT or MOSFET.

The main contributions to this publication were to perform a major part of the designing and building of the experimental setup, performing all experiments, loss and efficiency calculations and preparation of the manuscript.

1.7 Related Publications

The following publications include work related to a variety of aspects within the area of SiC devices, application and control of power electronics, which has been carried out along with this project, and where the author of this thesis has contributed.

In peer-reviewed journals

- D. Peftitsis, R. Baburske, J. Rabkowski, J. Lutz, **G. Tolstoy**, and H.–P. Nee, "Challenges regarding parallel connection of SiC JFETs", *IEEE Trans. Power Electron.*, vol. 28, no. 3, pp. 1449–1463, Mar. 2013.
- **G. Tolstoy**, B. Larsson, O. Wallmark, S. Norrga, H.–P. Nee, "Elimination of vector changes due to sector changes with DTC", *Accepted for publication in EPE Journal*, 2015.

In conference proceedings

- **G. Tolstoy**, D. Peftitsis, J.–K. Lim, M. Bakowski and H.–P. Nee, "Circuit modeling of vertical buried-grid SiC JFETs", *in Proc. of* 13$^{\text{th}}$ *International Conference on Silicon Carbide and Related Materials 2009*, ICSCRM 2009, pp. 965–968 , 11–16 Oct. 2009.
- J.–K. Lim, **G. Tolstoy**, D. Peftitsis, J. Rabkowski, M. Bakowski and H.–P. Nee, "Comparison of total losses of 1.2 kV SiC JFET and BJT in DC–DC converter including gate driver", *in Proc. of* 8$^{\text{th}}$ *European Conference on Silicon Carbide and Related Materials 2010*, ECSCRM 2010, pp. 649–652, 29 Aug.–2 Sept. 2010.
- D. Peftitsis, **G. Tolstoy**, A. Antonopoulos, J. Rabkowski, J.–K. Lim, M. Bakowski, L. Ängquist, and H.–P. Nee, "High-power modular multilevel converters with SiC JFETs", *in Proc. of IEEE Energy Conversion Congress and Exposition*, pp. 2148–2155, 12–16 Sep, 2010.
- D. Peftitsis, R. Baburske, J. Rabkowski, J. Lutz, **G. Tolstoy**, and H.–P. Nee, "Challenges regarding parallel-connection of SiC JFETs", *in Proc. of* 8$^{\text{th}}$ *IEEE International Conference on Power Electronics–ECCE Asia (ICPE ECCE)*, 2011 , pp. 1095–1101,30 May–3 Jun. 2011.
- D. Peftitsis, J. Rabkowski, **G. Tolstoy**, and H.–P Nee, "Experimental comparison of dc-dc boost converters with SiC JFETs and SiC bipolar transistors", *in Proc. of* 14$^{\text{th}}$ *European Conference on Power Electronics and Applications (EPE 2011)* 30 Aug.–1 Sept. 2011.
- D. Peftitsis, J.–K. Lim, J. Rabkowski, **G. Tolstoy**, and H.–P. Nee, "Experimental comparison of different gate-driver configurations for parallel–connection of normally–ON SiC JFETs", *in Proc. of* 7$^{\text{th}}$ *International Power Electronics and Motion Control Conference (IPEMC)*, 2012, vol. 1, pp. 16–22, Jun. 2012.

- **G. Tolstoy**, D. Peftitsis, J. Rabkowski, P. R. Palmer, and H.–P. Nee, "A discretized proportional base driver for Silicon Carbide Bipolar Junction Transistors", *in Proc. of* 5^{th} *IEEE Annual International Energy Conversion Congress and Exhibition (IEEE ECCE Asia Downunder)*, pp. 728-735, Jun. 2013

- P. Ranstad, F. Giezendanner, M. Bakowski, J-K Lim, **G. Tolstoy**, and A. Ranstad, "Power devices in a soft switching converter, including aspects on packaging", *ECS Transactions* 2014 64(7): 51-59

- **G. Tolstoy**, B. Larsson, O. Wallmark, S. Norrga, H.–P. Nee, "Elimination of vector changes due to sector changes with DTC", *in Proc. of* 16^{th} *European Conference on Power Electronics and Applications (EPE 2014)*, 26–28 Aug. 2014.

- D. Sadik, J. Colmenares, D. Peftitsis, **G. Tolstoy**, J. Rabkowski and H.-P. Nee, "Analysis of short-circuit conditions for silicon carbide power transistors and suggestions for protection,", *in Proc. of* 16^{th} *European Conference on Power Electronics and Applications (EPE 2014)*, 26–28 Aug. 2014.

- J. Colmenares, D. Peftitsis, **G. Tolstoy**, D. Sadik, H.-P. Nee, and J. Rabkowski, "High-efficiency three-phase inverter with SiC MOSFET power modules for motor-drive applications,", *in Proc. of IEEE Energy Conversion Congress and Exposition*, pp. 468–474, 14–18 Sep. 2014.

Chapter 2

SiC Power Devices and Applications

This chapter gives an introduction to SiC devices and exemplifies some applications that have been presented in the literature. Parts of this chapter have already been published in ***Publication I*** *and* ***Publication II****.*

The material properties of silicon carbide, compared to silicon, make SiC power switches devices for the future. Some of the properties of SiC, Si and GaN are seen in Table 1.1. The increased breakdown voltage enables SiC power devices to have higher blocking voltages than Si devices for the same ON-state resistance. The higher band-gap provides improved robustness to increased temperatures, while the higher thermal conductivity gives better possibilities to extract heat from the chip. Thus, enabling higher current densities. These properties are well known since several decades and are discussed in detail in for instance [21, 22].

The SiC technology enables three different design directions. These are:

- High-temperature design - Where cooling is impossible or very expensive. This can be used in, for instance down-hole drilling or space applications, [23, 24].

- High-frequency design - Where a high-frequency application is targeted, or as a way to reduce the size and cost of the passive components, as in the boost-converters operating at frequencies above 200 kHz presented in [25, 26].

- High-efficiency design - Where a high efficiency is targeted. An example is the 40 kW inverter with a efficiency exceeding 99.5 % presented in [27]. Another example is the 312 kW inverter targeted for vehicular applications presented in [28].

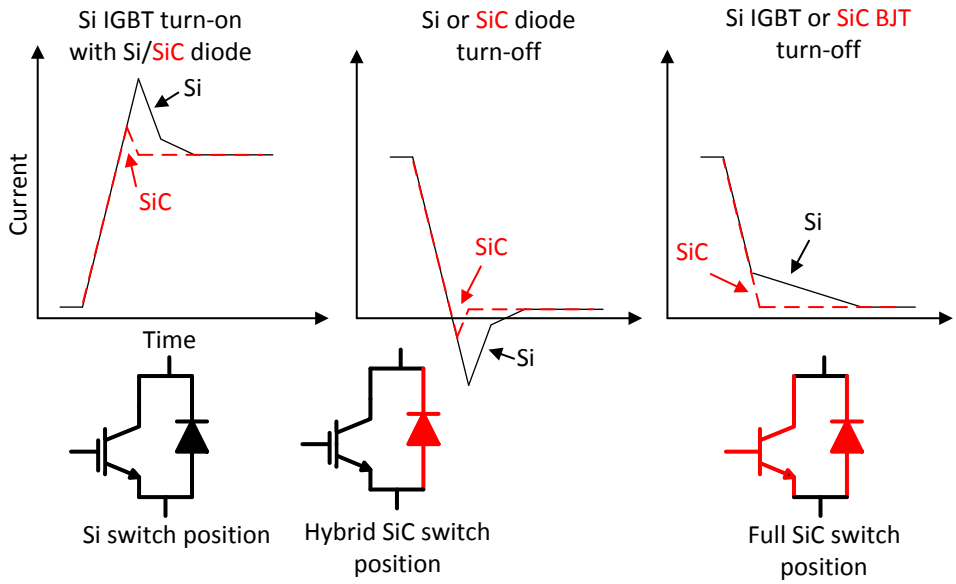

Figure 2.1: Benefit of SiC hybrid modules and full SiC modules compared to the all Si module.

The most common designs combine at least two of these to be able to attract a broader market. What is defined as high temperature, high frequency, and high efficiency is different for different applications and depending on the person making the definition. In general the reference is today's state-of-the-art silicon technology.

The Schottky diode was the first device to be adopted by the industry. The idea is to use them in, so called, hybrid modules, with a Si IGBT switch and an anti-parallel SiC Schottky-diode. This concept is able to reduce the switching losses substantially. The idea of the hybrid module can be seen in Fig. 2.1. The smaller reverse recovery of the SiC Schottky diode reduces the losses at both the turn-OFF of the diode itself, and also at the turn-ON of the Si IGBT. Some examples where hybrid modules are used are for instance: air condition applications, [29], inverters for smart grids [30], and traction applications, [31]. Furthermore, the hybrid module is beneficial to use whenever the Si IGBT utilizes hard turn-ON switching.

The next step is to adopt the so called "All-SiC" power modules. This will also reduce the losses from the turn-OFF transitions since SiC devices have essentially no tail-current.

2.1 SiC Power Devices

Today there are four main types of SiC switches that are available in large quantities. These are:

- normally-ON JFET
- normally-OFF JFET
- MOSFET
- BJT

For higher voltage ratings, up to 15 kV, the SiC IGBT is also of interest. It is now being tested in academia, [32, 33]. A review of these devices as well as their physical structures is presented in [5].

To drive an SiC device in an efficient way there are different considerations to be made for different devices. Some of these aspects are:

- Current or voltage driven device
- Unipolar or Bipolar device
- Normally-on or Normally-off
- Application

Table 2.1 shows some of the properties of the SiC power devices that have to be considered. The SiC JFET and the SiC MOSFET are unipolar devices, meaning that the conduction of current is based predominantly on the use of majority charge

Table 2.1: Properties of 1200 V SiC devices. (*There are many different structures for N-ON JFETs, some have usable body-diodes)

Device	**Control type**	**Reverse Conduction**	**Anti-parallel diode**
SiC BJT	Current controlled	Not possible	Full current rating of diode
SiC N-ON JFET	Voltage controlled	Yes	Usable body-diode or* diode for dead-time
SiC N-OFF JFET	Voltage and current controlled	Yes	Diode needed, rated for dead-time
SiC MOSFET	Voltage	Yes	Usable body-diode

carriers. Bipolar devices, on the other hand, make use of both the majority charge carriers and the minority charge carriers.

The unipolar devices are voltage controlled, even though the SiC JFET, especially the normally-OFF version [34], needs a current of 100-300 mA to the gate to reduce the resistance of the channel. The unipolar devices also have possibility to conduct the current in the reverse direction, [35]. The SiC MOSFET, and some of the normally-ON JFETs, have an intrinsic body diode. This body diode could be used to conduct the current during the dead-time. The voltage-drop across the body diode is much higher than that of an anti-parallel Schottky diode. It is not advisable to design a converter such that the body diode is used for the full duration of the reverse conduction. The temperature dependency of the ON-state voltage for the body diode of a lateral channel vertical JFET (LCVJFET) has been presented in **Publication I**. It is shown in Fig. 2.2a that the body diode of the LCVJFET has a negative temperature coefficient and is thus, not suitable for paralleling. However, the resistance of the channel has a positive temperature coefficient, as seen in Fig. 2.2b. This make the LCVJFET suitable for parallel connection if either an external anti-parallel diode is used or a correct dead-time control is utilized. The dead-time control of unipolar devices is discussed in Chapter 4.

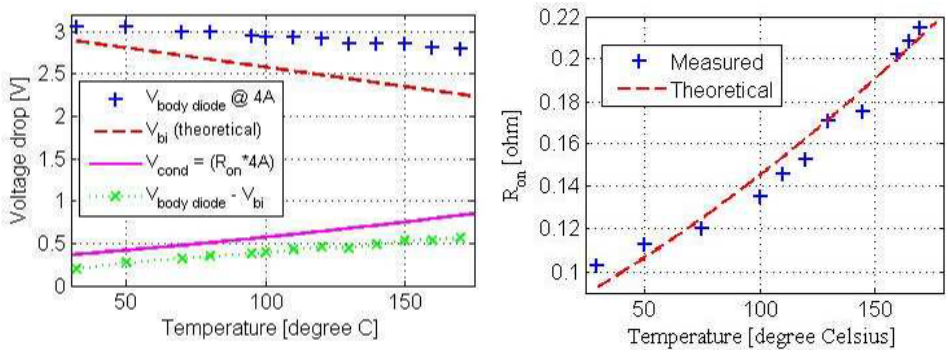

(a) (b)

Figure 2.2: (a) Voltage across body-diode and (b) ON-state resistance dependency of temperature.

A normally-ON JFET needs to have a negative voltage on the gate before the power to the system is supplied. Otherwise, a shoot-through current will occur which may destroy or degrade the devices. Some solutions to solve this have been presented in the literature. The self powered gate driver [36] and the *SiC JFET/Si MOSFET Cascode* [37] are two examples.

The SiC bipolar junction transistor is, on the other hand, current driven, cannot conduct any substantial current in the reverse direction, and does not have an intrinsic body diode. In most all other aspects, the SiC BJT behaves like a unipolar device with fast switching transients, resistive conduction losses and a positive temperature coefficient of the collector-emitter voltage. Since the SiC BJT is current driven, it is also a normally-OFF device.

devices have a positive temperature coefficient of the ON-state voltage drop above room temperature, [25, 27, 38], which is of great importance if parallel connection is targeted.

A non-scientific comparison between the popularity of SiC BJTs, SiC JFETs and SiC MOSFETs is shown in Table 2.2. It can be seen that the SiC MOSFET is by far the most popular device. There are three main reasons for that. Those are:

- The SiC MOSFET is the most developed device because it has had the most capital behind it. The companies that have developed the MOSFET have been able to have a long-term strategy.

- Engineers prefer the SiC MOSFET over the other devices since, from a driver point-of-view, it is the SiC device which most resembles the Si IGBT. The belief is, that it is only to exchange the gate driver voltages of the existing IGBT drivers and then the Si IGBT modules can be replaced with SiC MOSFET modules. This is of course possible, but it will not take full advantage of the more expensive SiC MOSFET modules.

- The SiC MOSFET is a normally-OFF device, meaning that the device is in the OFF-state if no power is supplied to the gate driver.

Table 2.2: Non-scientific comparison between the popularity of SiC components 26/4 - 2015

Forum and query	**SiC BJT**	**SiC JFET**	**SiC MOSFET**
IEEE XPLORE title: "SiC XXX"	32	101	94
IEEE XPLORE meta: "SiC XXX"	77	242	326
IEEE XPLORE meta: SiC and XXX	165	428	1137
Google: "SiC XXX"	7860	39900	151000
1200 V devices on Digikey	1	0	4

2.2 Why Silicon Carbide Bipolar Junction Transistors?

If the aspects from the previous section are taken into consideration, the question is: ***What niche does the SiC BJT fit into?***

– The SiC BJT is current controlled and needs considerable power provided from the base driver to conduct.

– The SiC BJT has almost no possibility to conduct the current in the reverse direction.

= The SiC BJT has approximately the same switching speeds as the SiC MOSFET and SiC JFET.

\+ In [39] it is found that at 125 °C the SiC BJT has the lowest specific ON-state resistance, which is the ON resistance normalized to the total chip area. The SiC BJT also has the smallest increase from 25 °C to 125 °C compared to a SiC MOSFET and three different types of JFETs. This indicates that the ON-state losses of the SiC BJT are less dependent on temperature than the other devices.

\+ The SiC BJT is a normally-OFF device, and since the BJT is current controlled it may not be as sensitive to crosstalk as the SiC MOSFET and SiC JFET. Both the unipolar devices have a low threshold voltage and are sensitive to crosstalk between the upper and lower switch in a half-bridge configuration. A solution to the crosstalk problem has been presented independently in [40] and [41].

\+ The SiC BJT has a great short-circuit capability [42]. This is due to the limit of the base current that brings the BJT device out of saturation and limits the shoot-through current. This is illustrated in Fig. 2.6 where short-circuit occurs for 1 μs for two different magnitudes of base current.

\+ The SiC BJT has no oxide-layer. The fabrication and stability of the oxide layer has been challenging for the SiC MOSFET. For the newer generations of MOSFETs the stability increases, but above 200 °C the SiC BJT is preferred [43].

The SiC BJT can be the device of choice in many applications. But it seems to excel in an environment where a robust device is needed that can withstand higher temperatures. It is yet to early to see what impact the 1200 V SiC BJT will have. It is possible that SiC BJTs finds its niche at higher blocking voltages. The high voltage SiC BJT seems to be promising at higher blocking voltages of 10 kV with

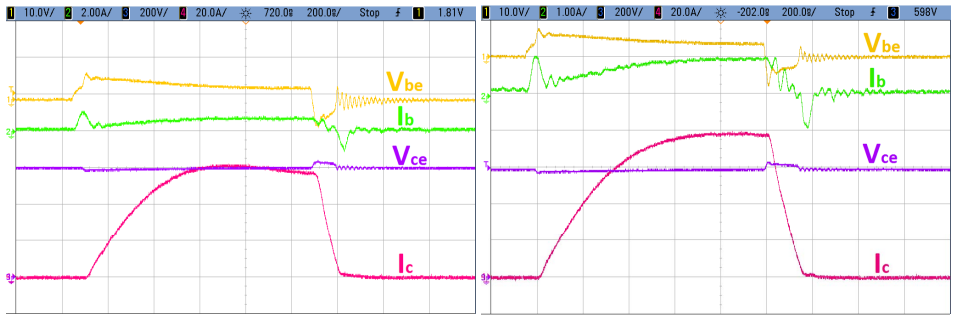

(a) (b)

Figure 2.3: SiC BJT short circuit currents for different base currents: (a) 0.5 A and (b) 1 A. Presented at EPE 2014, [42].

high gains of up to 75 as presented in [44]. Additionally, a 5.8 kV device with as low specific ON-state resistance as 28 $m\Omega cm^2$ has presented in [45].

Gain of Bipolar Junction Transistors

The SiC BJT is a current-driven device, which makes it stand out from the other devices. The gain, β, of the BJT is defined as

$$\beta = \frac{I_C}{I_B}, \tag{2.1}$$

where I_C is the magnitude of the collector current and I_B is the base current. The quantity β is defined as the ratio of the minimum value of I_B and I_C for the case when the device is fully ON. Typical gains for a 1200 V, 50 A SiC BJT, [46], as a function of I_C and the temperature are shown in Fig. 2.4. It can be seen that β is dependent on both the magnitude of I_C as well as the temperature.

Figure 2.5 illustrates what happens when the SiC BJT goes out of saturation. It shows the voltage and current waveforms of a SiC BJT in a boost converter. At a well-defined instant, the base current decreases discretely in the next two switching cycles. Three different switching cycles are shown with a base current that is reduced twice. During the first switching cycle the collector-emitter voltage, V_{CE}, drops at turn-ON and the current inductor current of the boost converter increases. For the next two cycles, the device never goes into saturation, and thus the full voltage is observed across the device. This shows the importance of supplying a sufficent amount of base current to the device.

How to drive the SiC BJT and related issues are discussed further in Chapter 3.

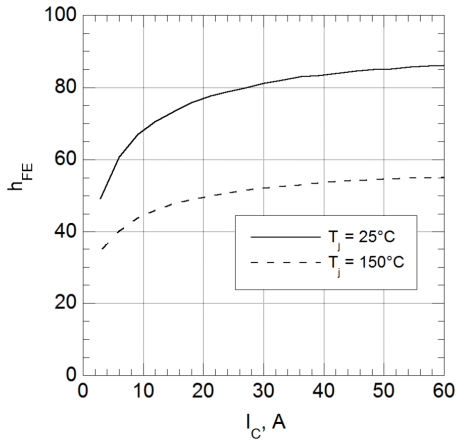

Figure 2.4: Gain of SiC BJT from Fairchild presented in [46] with permission of the author.

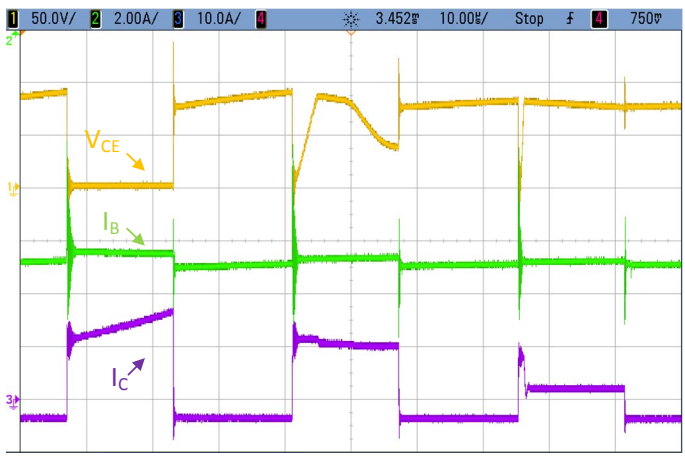

Figure 2.5: Collector-emitter voltage (top), base current (middle), and collector current (bottom) when reducing the base current in steps.

2.3 Applications for SiC power devices

The initial rating of the blocking voltage for the majority of SiC transistors when appearing on the market was 1200 V. At this blocking voltage there is no competition from Si MOSFETs, only from Si IGBTs. Even though the hybrid modules are found in converters and systems today, not many “All SiC” products have yet

been commercialized. However, lots of work is performed all across the world in both industry and academica by several research groups. This section gives some examples of applications that have been proposed:

- **Automotive applications** One reason to limit the devices to 1200 V is the influence of the automotive industry. In the last decade a tremendous development has occurred in hybrid electric vehicles (HEVs). The higher efficiency of SiC power electronics enhances the range of the vehicle while the lower losses and higher temperature tolerance give the opportunity to reduce the cooling system, and makes the drive system both lighter and cheaper. The gain of 1200 V SiC JFETs over 1200 V Si IGBTs is exemplified for HEVs in [47] and in January this year, Toyota announced that they are testing an Toyota Camry with SiC devices in the drive train of the car.

- **Railway traction** also shows great potential for SiC devices [31]. Last year Mitsubishi released an "All SiC" 3.3 KV, 1.2 kA module for railway traction applications. It is stated to enable both a reduction of size and increase in efficiency.

- Converters targeted for **photo voltaic (PV)** applications have shown great potential. PV systems need several switch-mode converter steps to transform the electricity to the grid. To reduce the overall losses, converters based on SiC devices could be used [26, 48].

- **Resonant converters** for induction heating is another filed with an extensive development, [49, 50]. There are many new ideas and realizations of old ideas that did not work with Si IGBTs. Chapter 4 discusses several aspects of SiC power electronics in resonant converters. Resonant converters can be used for other applications as well.

- High-efficiency **AC drives** is another area with potential. Here high-efficiency together with compact design is of importance [27, 28].

The list can easily be made longer. The point is, that when the SiC technology has matured, it has shown its reliability and prices have come down, it may be of interest in all applications that need devices with a blocking voltage of 1200 V or higher. However, there have to be at least a few main applications where the technology can show its maturity. It will be interesting to see if the Mitsubishi traction converter is successful. Another area in which the author foresees a large and early impact of the SiC technology is high-frequency resonant converters. Higher frequencies than today are achievable, which open the field to thin materials as well as to non-magnetic materials.

High Voltage Direct Current

One future area of power electronics where the high-voltage SiC devices, 3.3 kV and above, will have an impact is in HVDC transmission. Since HVDC transmission transfers high power, an increase in efficiency of just 0.1 % – 0.2 % is of great importance. A theoretical study was made in **Publication II** to investigate the impact that SiC JFETs and SiC BJTs could have in a modular multilevel converter (M2C). For the M2C application the SiC JFET have two major advantages over the SiC BJT:

- The SiC BJT needs a significant base current. For the high power that M2C is targeting the base drivers will consume a significant power. This power consumption can be reduced with proportional base drivers which are discussed in Chapter 3.

- The SiC JFET has the possibility to conduct the current in reverse direction. This will reduce the ON-state losses compared to conducting the current through the ant-parallel diode.

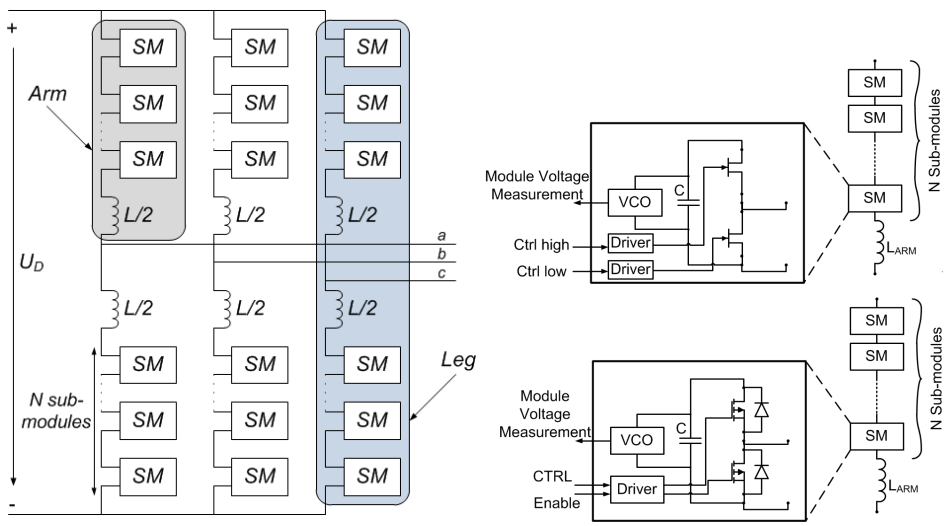

Figure 2.6: (a) Schematic of M2C and (b) submodule design of the experimental setup with a SiC JFET (top) and of a Si MOSFET and its anti-parallel diode (bottom).

Figure 2.6a shows the schematic of the M2C. The concept of M2C is that you can switch in and out discrete voltage sources to get a more sinusoidal voltage waveform than a 2-level converter. The M2C concept is described in [51].

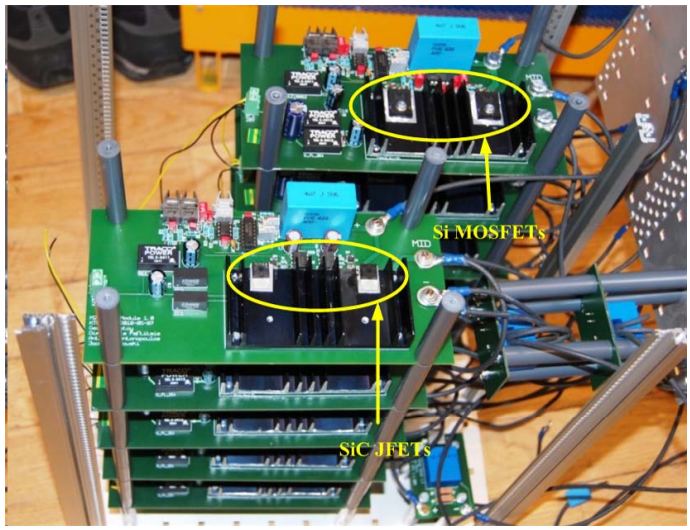

Figure 2.7: Phase leg of the lab prototype showing the SiC and the Si submodules.

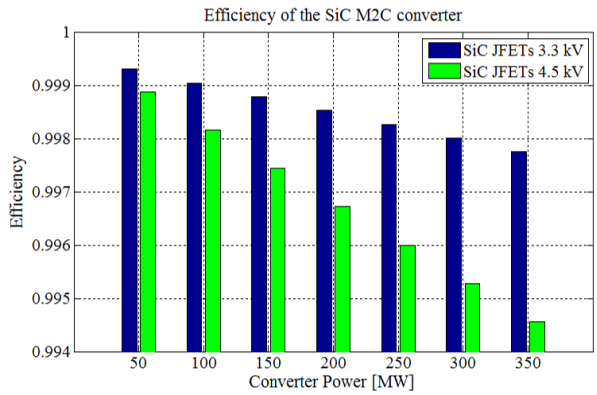

Figure 2.8: Comparison of the SiC M2C efficiency for both the SiC JFET cases.

A comparison to a corresponding M2C with Si IGBTs, [51], was conducted. A submodule of a down-scaled 3 kVA prototype M2C was replaced with a submodule with SiC JFETs without anti-parallel diodes. This was the same SiC LCVJFET as

the one characterized in **Publication I**. These submodules are seen in the schematic diagram of 2.6b, and a photography of the setup is seen in 2.7. It is shown that the diode-less operation is possible with the JFETs conducting in the negative direction, leaving the possibility to use the body diode during the switching transients. Experimental waveforms for the SiC submodule verify the feasibility during normal steady-state operation. In Fig. 2.8 the calculated losses for two high-voltage JFETs are shown. The loss estimation shows that a 300 MW M2C for high-voltage direct current transmission would potentially have an efficiency of approximately 99.8% if equipped with future 3.3 kV 1.2 kA SiC JFETs.

This chapter has discussed the various existing SiC devices and shown some potential industrial application for the SiC technology. Additionally, a brief summary of the results from **Publication I** and **Publication II** is presented. In the next chapter, different base driver concepts for SiC power BJTs are presented.

Chapter 3

Base Drivers for Silicon Carbide Bipolar Junction Transistors

This chapter builds on the results presented in ***Publication III*** *and* ***Publication VI****.*

Optimizing base drivers is one way to make the SiC power BJT more attractive for customers who seem to prefer the more easily driven SiC MOSFET. One way of optimization is to reduce the power consumption of the base driver while keeping the steady-state and switching performances. This chapter summarizes the published base drivers for SiC power BJTs with a focus on the appended papers. Section 3.2 presents the results from **Publication III**, where the dual-source driver is introduced. This section also discusses other driver concepts that have been presented. Section 3.3 introduces the proportional base drivers and especially the results in **Publication IV**, which is the publication where the first proportional base driver for SiC BJTs were published.

Finally, in Section 3.4, the reverse conduction properties of the SiC BJT and the relation to the base driver are described as in **Publication VI**.

3.1 Introduction to Base Drivers

Even though the gain for the SiC BJT is an order of magnitude higher than for the Si BJT, [52, 53], and that most of the other drawbacks from Si BJT era have been eliminated, [46, 54], there is not as much interest in the SiC BJT as it is for the SiC JFET or the most popular SiC MOSFET as was shown in Table 2.2. This is mostly due to the two main drawbacks of the SiC BJT compared to the the SiC MOSFET and SiC normally-ON JFET. These are the inability to conduct the current in the reverse direction and that a fairly high on-state base current is needed to drive the

device into saturation.

The first drawback has an easy solution: to use an anti-parallel diode. This is done for Si IGBTs and is also used today in most, if not all, SiC MOSFET modules [55]. When the SiC BJT and its anti-parallel diode conducts a current in the reverse direction, an increased voltage drop is observed compared to the forward conduction. A look at the data-sheet from CREEs SiC MOSFET module CAS300M12BM2, rated for 300 A and 1200 V, shows that the voltage drop across the diode at 300 A is 1.7 V with a negative gate voltage. If instead a positive gate voltage of 20 V is applied, thus enabling reverse conduction through the channel, the voltage drop is lowered to 1.2 V. At 100 A the difference is even larger with voltage drops of 1.2 V and 0.5 V. Almost the full current goes through the channel of the MOSFET instead of significantly sharing with the anti-parallel diode. This gives higher losses for the system built with BJTs and anti-parallel diodes. The BJT system also needs the diodes to be rated at the full current which means more SiC used. The unipolar devices just need to rate the diodes for the duration of the dead-time. This was shown for a 40-kW converter using 10 parallel JFETs and just a single Schottky-diode in each switch position, [27]. For some of the unipolar devices there is the possibility to use the inherent body-diode instead of an additional Schottky-diode. This has been investigated in a resonant converter [**Publication VI**] using a CREE 25 mΩ MOSFET without any anti-parallel diode and for a 100 mΩ JFET operating in a modular multilevel converter, [**Publication II**]. This was first shown by Ållebrand in 2001, [56].

A way to eliminate this drawback is to use the SiC BJT in converters where the current only flows in one direction, like a one-directional boost converter. This has been described in [25, 57].

The second drawback, a fairly high on-state base current, is on the other hand something that can be minimized by optimizing the base driver. And this is what will be discussed in this chapter.

3.2 Base Drive Concepts

Power bipolar junction transistors, or Power BJTs, have been around since the 80's and thus, there are at least three different concepts for the base drivers. However, as was shown in the review of Si BJT base drivers made in **Publication III**, the issues that the base driver designers faced with the Si BJTs are not relevant for SiC BJTs. The review shows three types of base drivers that were commonly used:

- Direct drivers with Baker clamp and speed-up capacitors [8, 58].
- Drivers for Darlington transistors [52, 58, 59].

- Proportional drivers with collector current transformers [58, 60].

All these drivers were complicated in comparison with state-of-the-art IGBT drivers of today, and even though some ideas from the 80's could be re-used a new design had to be made for the SiC BJTs.

The two main design criteria for a base driver of a SiC BJT are:

1. Enable fast switching of the device by providing and extracting the base charge sufficiently fast.

2. Provide sufficient base current to keep the device in saturation during the on-state.

This should be done while consuming as little power as possible, being able to keep the device off during the OFF-state and have low oscillations on the base.

The different contributions to the driver power consumption are identified. From the device itself two consumptions can be derived. During steady-state conduction the base current, I_B, consumes power, P_{BE}, across the base-emitter junction,

$$P_{BE} = I_B * V_{BE}, \tag{3.1}$$

where V_{BE} is the voltage drop across the base-emitter junction. This voltage is fairly stable during forward conduction and varies slightly with temperature and collector current. The second driver consumption from device the itself is related to the charge that must be provided to the base, P_{SB}. The corresponding power is given by

$$P_{SB} = Q_B * V_{BE} * f_S, \tag{3.2}$$

where f_S is the switching frequency of the device and Q_B is the base charge. P_{SB} in (3.2) is independent of which driver design is used while P_{BE} in (3.1) is approximately linearly dependent on the base current.

It is important to ensure that the device turns on and off sufficiently fast to minimize the switching losses. Even though there is a relation between reduced switching losses and increased driver consumption, it is more important from a systems point-of-view to keep the switching losses low instead of keeping the driver consumption to a minimum.

Single-Source Base Driver

In [**Publication III**] a simple approach is followed by testing a single-source driver and identifying where the power consumption of the driver originates from and

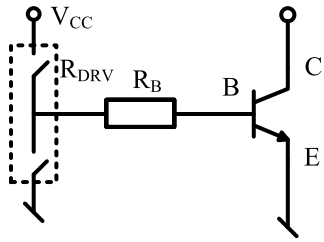

Figure 3.1: Single-source base driver with base resistor.

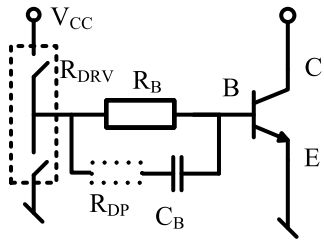

Figure 3.2: Single-source base driver with speed-up capacitor and optional damping resistor.

calculating the losses. The two single-source concepts can be seen in Fig. 3.1 and Fig. 3.2.

These simple concepts are well known. The first driver consists of a voltage source, V_{CC}, a totem-pole and a base resistance, R_B. This driver has resistive losses, P_R, in R_B and in the resistive channel of the totem-pole, R_{DRV}, during conduction,

$$P_R = I_B^2 * (R_B + R_{DRV}). \tag{3.3}$$

The second driver also has a speed-up capacitance, C_B, for faster transients. A damping resistor, R_{DP}, can be used to damp out the introduced oscillations. The introduced speed-up capacitor causes power consumption, P_{CB}, as it is charged and discharged during transitions. This consumption is derived as,

$$P_{CB} = (V_{CC} - V_{BE})^2 * C_B * f_S, \tag{3.4}$$

where $(V_{CC} - V_{BE})$ is the voltage that the capacitor is charged to during turn-ON. Two other consumptions are added to take the total consumption into considerations. These are $P_{STANDBY}$ which is the losses of the driver when there is no base current flowing and no switching occurring of the device. This consumption

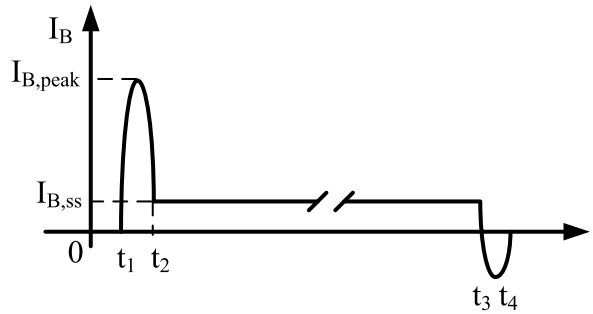

Figure 3.3: Ideal base current.

comes from the isolated supply, the fiber receiver or opto-coupler, and other passive consumption that has no direct impact on the driving of the device. Finally, there are additional losses, P_{ADD}, which are the losses that are hard to measure and calculate. P_{ADD} usually become larger with a higher base current and a higher switching frequency.

For the steady-state consumption a low V_{CC} is preferable, since that enables a small R_B, minimizing P_R in (3.3). However, on the other hand, a high V_{CC}, in combination with a speed-up capacitor makes the turn-ON and turn-OFF of the SiC BJT faster, enabling lower switching losses and a higher switching frequency. These two attributes are hard to combine in a single-source driver.

A solution is presented in the next section, a dual-source (2SRC) base driver.

Dual-Source Base Driver

The 2SRC base driver, that was first introduced in [**Publication III**], combines a low steady-state base current together with a high base current during transients for fast switching. The ideal waveform of the base current is shown in Fig. 3.3. It is possible to achieve this current shape with a number of different drivers, [61, 62] are two different examples that have been published.

The 2SRC base driver is shown in Fig. 3.4 and consists of two totem-pole drivers that are connected to different voltage sources, one low-voltage source for steady-state operation and a high-voltage source that is optimized for the transients. A base resistor limits the base current in the steady-state part, while a capacitor is used on the high-voltage side to supply transient current to the base during turn-ON as well as to extract the charge of the base during turn-OFF. This driver is more complicated than a single-source driver, but on the other hand, it performs much better. A comparison can be seen in Table 3.1, where the consumption comparison

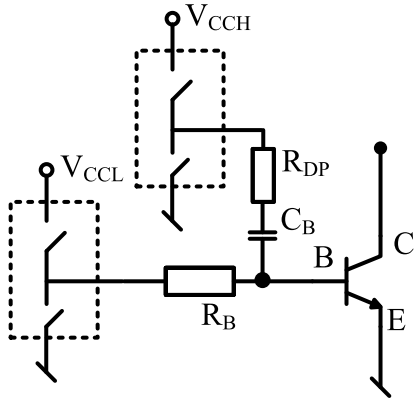

Figure 3.4: Dual source, 2SRC, base driver.

is calculated with a duty ratio of 0.5 and a switching frequency of 100 kHz.

The 2SRC base driver turns on and off the device much faster than the single-source drivers just using a 5 V supply. The 2SRC base driver should be used instead of the single-source drivers if a high-frequency hard-switching application is targeted. For soft-switching applications, on the other hand, the simpler R-C network base driver could be used.

Figure 3.5 shows the base driver consumption for the 2SRC base driver concept at different frequencies. It can be seen that at higher frequencies, 200 kHz and above, the driver consumption associated with the switching transitions becomes a more dominant factor and has to be considered. The 2SRC base driver concept was used when a compact boost converter with a rating of 6 kW was constructed [25].

Table 3.1: Driver comparison. Consumption is at D=0.5 and f_s=100 kHz.

Driver	**Resistor**	**R-C Network**	**2SRC**
V_{CC}	5 V	5 V	5/24 V
R_B	5.6 Ω	5.6 Ω	5.6 Ω
C_B	-	68 nF	6.8 nF
P_{CB}	-	27 mW	300 mW
$P_{CB} + P_R + P_{BE} + P_{SB}$	815 mW	842 mW	1115 mW
t_{ON}	350 ns	110 ns	20 ns
t_{OFF}	100 ns	45 ns	35 ns

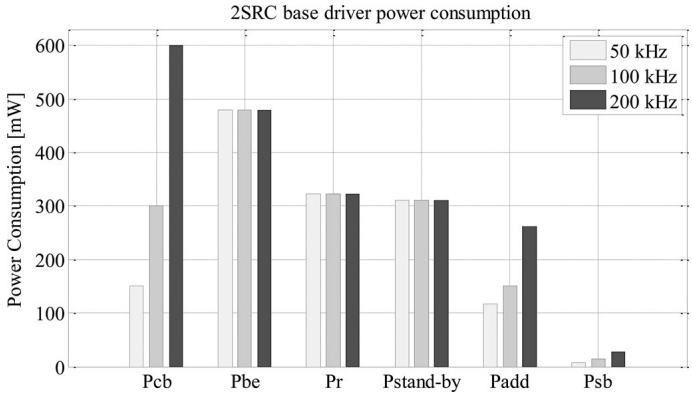

Figure 3.5: Driver consumption for the 2SRC base driver at different switching frequencies.

One of the aims of this publication was to see how small the passive components could get with a switching frequency of 250 kHz. At this high frequency, the drivers needed dedicated forced cooling.

3.3 Proportional Base Driver Concepts

This section focuses on different concepts to reduce the steady-state consumption of the base driver. The idea behind this is that the load current for most applications varies over time, and especially the current that flows through the BJT, and thus the base current could be varied over a load cycle. This will reduce the total consumption of the base driver. The driver would still need to be designed to deliver base current for the maximum collector current and temperature of the application. The gain of the SiC BJT is dependent on the temperature and the collector current as explained in Chapter 2.

The idea of proportional drivers for BJTs is not new, but was used, or at least presented in scientific journals, for Si BJTs in the 80's. None of these ideas where applicable to switch a SiC BJT in an efficient way. One concept was to add a transformer on the collector side to have a direct feedback to the base driver. Since SiC devices can switch very fast current transients, it is not advisable to add an additional inductance in the current path. Two main current source concepts for proportional drivers for SiC BJTs have been presented. One is a pulse-width modulated (PWM) solution, Fig. 3.6, and the other is based on combining fixed current sources, Fig. 3.7.

The PWM-based solution, that was presented in [63] (which is a conference

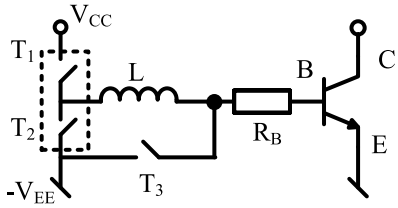

Figure 3.6: Pulse-width modulated proportional base driver concept for SiC BJTs.

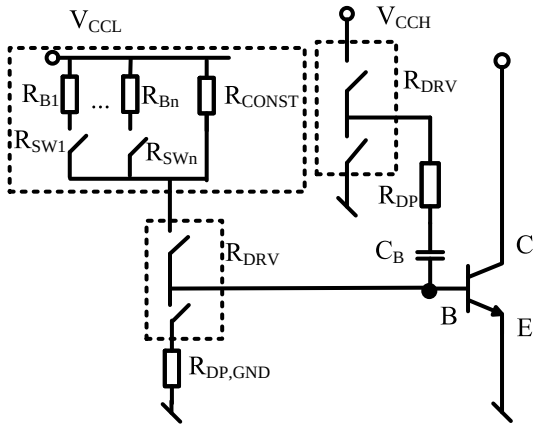

Figure 3.7: Proportional base driver voltage source concept, with a variable resistor bank. This driver is also known as discretized proportional base driver (DPBD).

publication that had this part removed when reworked into **Publication IV**), has few passive components and reminds of the concept presented in [62]. It employs the same idea for fast turn-ON, but then T1 and T2 are operated by means of PWM to adjust the current within a certain tolerance band such that the SiC BJT is kept in saturation mode. This concept has been presented for a soft-switching application, [64], with good results. But in, [64], the base driver control did not include the possibility to energize the inductor before turn-ON in order to achieve a fast turn-ON.

The discretized proportional base driver (DPBD) seen in Fig. 3.7 is based on the ideas from the 2SRC driver but with the possibility to adjust the base current depending on the demand. The driver uses the possibility to switch in and out discrete current sources to adjust the base current. For the highest base current all current sources, R_{SWx}, are switched in, and when the collector current is very low, only R_{CONST} is conducting.

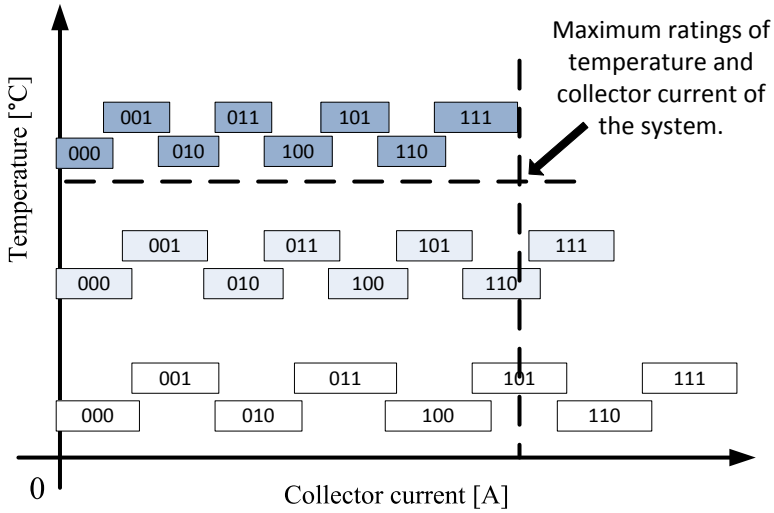

Figure 3.8: Proposed control of the DPBD with eight different base current levels.

Discretized Proportional Base Driver (DPBD)

Control of DPBD

To be able to control the base current in accordance with the collector current and temperature, both those quantities have to be measured. In some applications, just one of these quantities might change. For instance, if the temperature of the switch is constant or if the collector current is close to constant. An illustration of the proposed control can be seen in Fig. 3.8, where eight different base current levels are available and the temperature range is divided into three discrete levels.

The control works in such a way that, when the collector current increases, the base current increases from one discrete level to the next on the right. For example, from 001 to 010. As the temperature increases, the range for each discrete level is reduced due to the lower gain. Two look-up tables are used, one to see if the upper limit of the collector current is reached, H-LUT, and one to see if the lower limit is reached, L-LUT. The number of columns in each control table is one less than the number of discrete base current levels and the number of rows is how many discrete temperature levels the control has been divided into. As can be seen in Fig. 3.8 the current levels overlap. This enables the hysteresis control function.

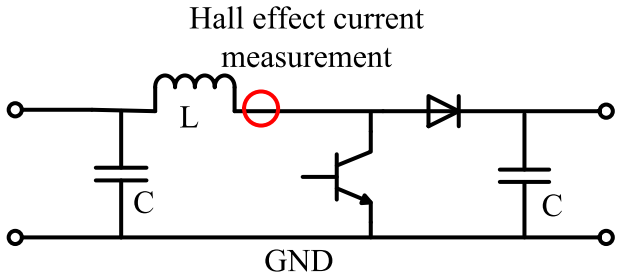

Figure 3.9: dc-dc boost converter with a Hall-effect current measurement.

Implementation of DPBD

The DPBD is designed and the control is implemented for a boost converter. The inductor current is measured by a Hall-effect current sensor as shown in Fig. 3.9. The output from the Hall-effect current measurement is then fed back to the controller to be used as the input for H-LUT and L-LUT. In the implementation, only one temperature level is used. The numbers in the H-LUT and L-LUT tables, seen in Table 3.2 represent the output voltage from the Hall-effect current sensor in mV. If the index is 0, and the control value increases above 900 mV the index changes from 0 to 1. To change the index again, the control voltage has to increase above 1200 mV or under 800 mV. Figure 3.10 and Table 3.2 show the calculated and measured consumptions for different base currents with $f_S = 98$ kHz and $D = 0.6$ at room temperature. The steady-state consumption, $P_R + P_{BE}$, increases linearly with the base current. The steady-state consumption increases seven times wile the total consumption of the DPBD more than doubles when the base current increases from 0.18 A to 1.27 A.

The blue crosses in Fig. 3.10 show the measured consumption of the DPBD

Table 3.2: Control Arrays H-LUT and L-LUT, base current, calculated steady-state losses and measured losses at 98 kHz and $D = 0.6$

Index	0	1	2	3	4	5	6	7
Switch control	000	001	010	011	100	101	110	111
H-LUT	900	1200	1500	1800	2100	2400	2700	-
L-LUT	-	800	1100	1400	1700	2000	2300	2600
Base current [A]	0.18	0.48	0.71	0.87	1.04	1.13	1.21	1.27
Calculated P_R	0.22	0.57	0.85	1.04	1.25	1.36	1.46	1.53
Calculated P_{BE}	0.33	0.86	1.28	1.56	1.88	2.04	2.18	2.29
Measured con. [W]	2.82	3.86	4.51	5.21	5.67	6.17	6.36	6.61

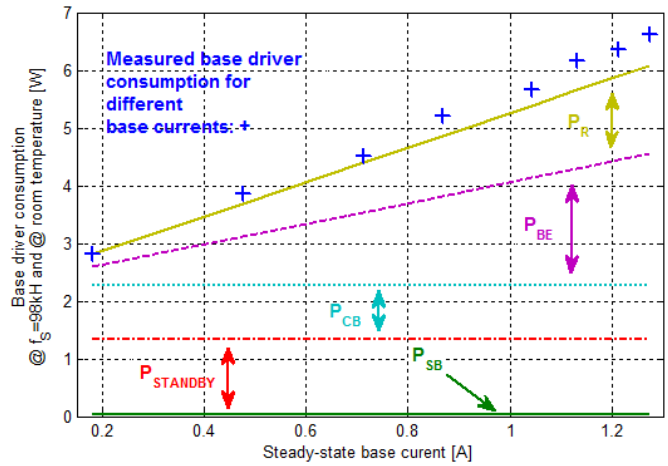

Figure 3.10: Measured base driver consumption versus calculated base current consumption for different base currents.

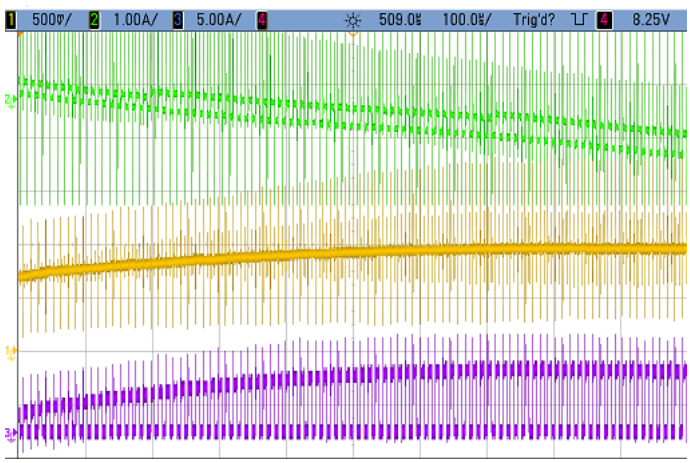

Figure 3.11: Base current (top), Hall-effect output voltage (middle), and collector current (bottom) just after switching has started. f_S = 91 kHz and D=0.6.

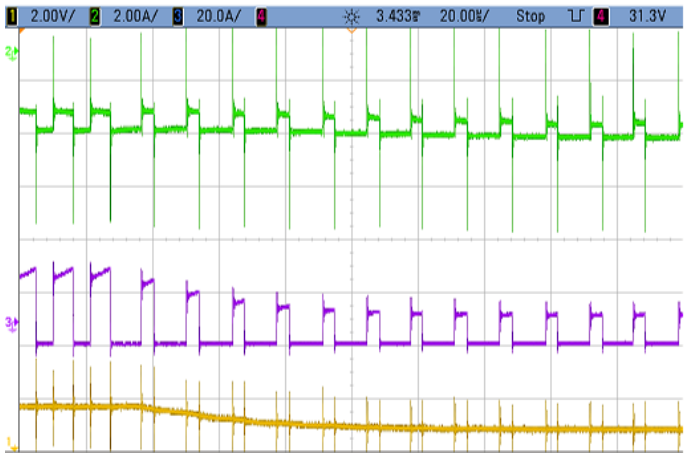

Figure 3.12: Base current (top), collector current (middle), and Hall-effect output voltage (bottom) as the duty-ratio changes from 0.6 to 0.38.

for different discrete values of the base current. The measured consumption agrees well with the calculated consumption.

A Hall-effect-based linear current sensor is used in series with the inductor to measure the inductor current. Hall-effect element implemented in the circuit transmits a voltage whose magnitude depends linearly on the inductor current. This voltage is then measured and averaged in a digital signal processor (DSP) shortly after turn-OFF transients have passed in the inductor current. The DSP then uses two simple arrays to decide if the inductor current has changed enough in either direction to warrant a change in steady-state base current for the next ON-state interval for the SiC BJT in the boost converter. If a change is detected in H-LUT or L-LUT then the base resistor switches are switched before the BJT turns on again. Figure 3.11 shows the base current, collector current and Hall-effect output voltage just after the boost converter has started to switch with a duty-ratio of 0.6. It can be seen that the collector current increases from its initial state. As the collector current increases, so does the inductor current which is measured by the Hall-effect transducer. When the control signal increases, so does the base current. It can be seen that the base current increases twice during the period seen in the oscilloscope screen dump. The currents are measured by Rogowski-coils which integrate the measured voltage. A Rogowski-coil captures fast transients very well but cannot reproduce direct currents. This is the reason for why the average

value of the base current reduces over time. In Fig. 3.12, the duty-ratio changes from 0.6 to 0.38. This reduces the collector current and also the Hall-effect output voltage, which in turn reduces the base current.

Applications for the Proportional Driver

Table 3.3: Steady-state energy consumption during the NEDC. $D = 0.5$, $T_J = 145°C$

Energy consumption	Boost simple drive	Boost DPBD with 4-I_B lvls	Buck simple drive	Buck DPBD with 4-I_B lvls
$\int P_R dt + \int P_{BE} dt$	2242 J	834 J V	774 J	311 J
$\int P_{ON-state} dt$	1353 J	1353 J V	687 J	687 J

The possibilty to reduce the losses in the proposed driver depends on how many levels are chosen for the base current and on the waveform of I_C. This driver will reduce the steady-state losses in applications where the collector current of the BJT varies over time. To make a comparison of the loss reduction with the introduced discretized BJT driver and the one with a constant base current, a simulation has been made of an ideal electric vehicle driving the standard drive cycle *New European Driving Cycle* (NEDC). The application is a dc-dc converter that transfers the energy from a 400 V battery to a 800 V dc-link or vice versa during breaking. The steady-state energy consumption can be seen in Table 3.3. The total base driver consumption of both drivers are compared with the ON-state losses of the SiC BJT. It is interesting to note that the driver consumption is in the same range as the losses from the device.

3.4 Reverse Conduction of SiC BJTs and the Relation to Base Drivers

Reverse conduction for the SiC BJT has not been fully investigated in the literature. This subsection is taken from **Publication VI** and aims to shed some light on this issue. The reverse conduction properties of SiC JFETs and SiCMOSFETs are well known and is presented, in for instance, in **Publication I** and [35].

For Si BJTs unreasonably high base currents where observed during reverse conduction as described in [8]. The paper, which is from the 80's, describes possible problems with different base drivers such as Darlington drivers and direct drivers. The main issue was the reduction of V_{BE} during reverse conduction of the Si BJT

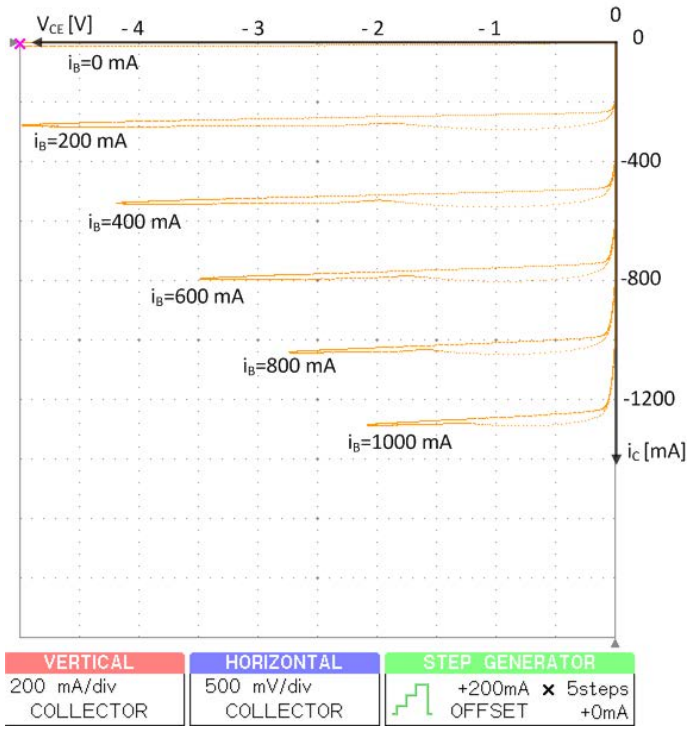

Figure 3.13: Tracer graph showing collector-emitter voltage versus collector current for different base currents, using steps of 200 mA.

and its anti-parallel diode. Due to the lower V_{BE} a higher voltage was obtained across the base resistance and thus a higher base current was obtained.

For the SiC BJT, as for the Si BJT, V_{BE} is not constant but depends on the voltage drop across the BJT and its anti-parallel Schottky-diode. For instance, with 0 V applied across the SiC BJT V_{BE} is 2.82 V at room temperature using a base current of 0.615 A. If a current of 10 A is a applied to the device V_{BE} increases up to 2.91 V. However, if instead a reverse current with a sufficient magnitude to push the device out of saturation is applied, then V_{BE} is a function of the voltage drop across the diode. With a reverse current of 0.75 A and a base current of 0.64 A the device is still in saturation but when a higher reverse current is applied the device comes out of saturation and the diode starts conducting. This in turn reduces V_{BE}. [65]

To investigate the reverse conduction of the SiC BJT a curve-tracer was used. The reverse gain, β_R, is approximately 1.2, as shown in Fig. 3.13. As seen in Fig.

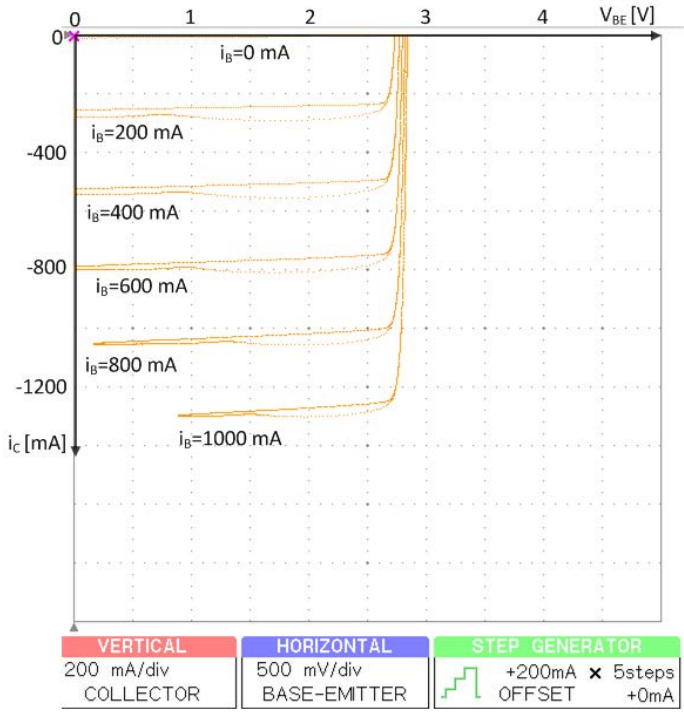

Figure 3.14: Tracer graph showing base-emitter voltage versus collector current for different base currents, using steps of 200 mA.

3.14, V_{BE} is stable as long the device is in saturation mode. But when a negative voltage is applied across the collector-emitter junction, like in the case of anti-parallel diode conduction, the BJT will no longer operate in the saturated mode, as seen in Fig. 3.13. To further illustrate what occurs when the SiC BJT has base current flowing during reverse conduction can be seen in Fig. 3.15. The uppermost trace is the current that flows through a BJT and its anti-parallel Schottky diode. In this figure the current, I_{EC}, is defined in defined in the opposite way than the normal convention for the collector current. This means that a positive value indicates a current flow from emitter to collector. The middle trace is V_{BE} and the trace at the bottom is I_B. It can be seen that when I_{EC} is going to zero V_{BE} increases. This means that the voltage across R_B, in the 2SRC base driver, is reduced and thus a smaller base current flows to the base. Since β_R is approximately 1.2 the SiC BJT goes into saturation before the zero-crossing.

This phenomenon, that V_{BE} is reduced during reverse conduction, has to be taken into consideration when designing a base driver. SiC BJT drivers usually

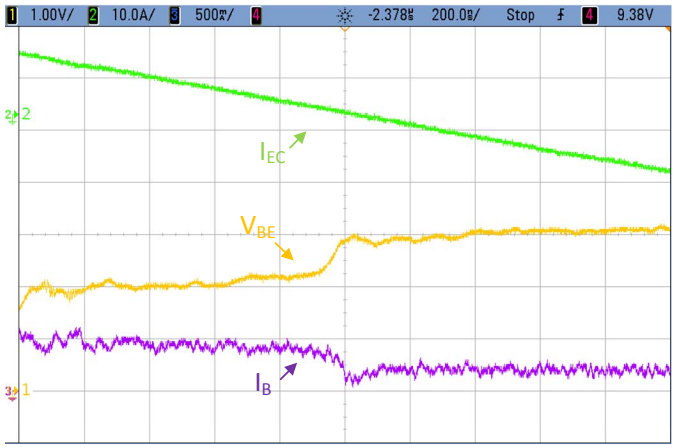

Figure 3.15: Current through the switch position defined in the emitter-collector direction, I_{EC} (top), V_{BE} (middle), and I_B (bottom) before and after the zero-crossing of the current.

have a steady-state design that considers a constant V_{BE} and then a resistor is used to set the base current to a desired level. The base-driver losses might be significantly higher than expected due to the higher base-current. Thus, if not properly dimensioned, the electronics of the base driver can be damaged due to the higher currents and increased temperatures. Three ways to reduce this problem are proposed:

1. Use a control algorithm that makes sure the BJT only conducts in the reverse direction just before the collector current goes through zero.
2. Make sure that the base driver can withstand the increased power dissipation.
3. Use a proportional driver that sets the base current to a minimum during reverse conduction.

In [**Publication IV**] the two first solutions are tested and compared in a resonant converter. A significant reduction of the steady-state power consumption, $P_R + P_{BE}$, of the base driver is achieved. This is discussed further in Section 4.4.

This concludes the chapter on base drivers and the aspects of driving the SiC BJT during reverse conduction. In the next chapter the impact of the SiC BJT and SiC MOSFET in a series-resonant converter is presented.

Chapter 4

SiC unipolar and bipolar power devices in a SLR converter

This chapter compares the performance of the SiC unipolar (MOSFET) and bipolar (BJT) devices in an SLR converter where efficiency and high-frequency operations are studied. Six different aspects have been considered. The results in this chapter are presented in ***Publication V*** *–* ***Publication VIII****.*

Finding the applications where SiC power devices can have the greatest impact is important. One of the applications where SiC could have a great and early impact is in resonant converters. This is due to that the fact that the fast switching transients and the lack of tail-current makes it better suited to for use in soft-switching applications. The switching loss of the SiC power switches are much smaller compared to the Si IGBT. This enables very high switching frequencies. This chapter summarizes the investigation of introducing the SiC power devices in the full-bridge series-loaded resonant (SLR) converter.

Six different aspects were investigated, and how the losses in the SiC power devices are affected by them:

- Load voltage - For all tests, the load voltage was varied in steps as a percentage of the dc-link voltage, i.e. 0, 25, 50, 70, and 90 % .

- Device - Two different devices were investigated: A unipolar SiC MOSFET with body diode and a bipolar SiC BJT with an anti-parallel SiC Schottky diode.

- Dead-time - An active dead-time control and how it affect the bipolar and unipolar SiC power devices was investigated?

- Switching frequency - To be able to vary the switching frequency, three different resonant tanks were used.
- Capacitive snubber - For each resonant frequency, different values of snubber capacitance were investigated.
- Control method - All tests, except one, are done with frequency modulation (FM). Dual control (DuC), [66], is investigated as an alternative control method. DuC is believed to be very beneficial together with SiC unipolar devices.

4.1 Basics of the SLR Converter with Capacitive Snubbers

The basic full-bridge SLR converter, Fig. 4.1, consists of a full-bridge which has its output loaded with a resonant tank. The latter consists of an inductor, L_{RES}, and a capacitor, C_{RES}, in series with a load. Typically, a dc-load is fed by a rectified current from a isolation transformer. If a high-frequency load is targeted, i.e. induction heating, [50], then no rectification is needed.

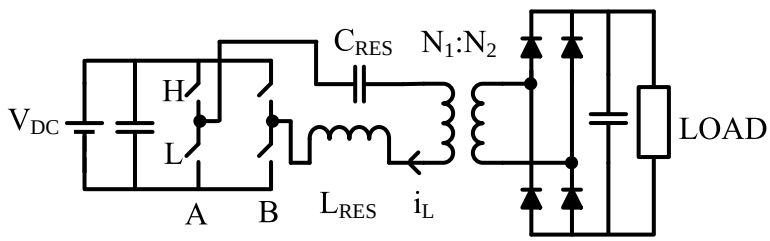

Figure 4.1: Typical SLR converter with diode rectifier.

The resonant tank has minimum impedance at

$$f_0 = \frac{\omega_0}{2\pi} = \frac{1}{2\pi\sqrt{L_{RES} * C_{RES}}}, \tag{4.1}$$

where f_0 is the resonant frequency of the tank.

The control of the SLR converter can be done with different control methods. The most common are frequency modulation (FM) and phase modulation (PM). Additionally, dual control has been suggested. These control methods are explained in detail in [66].

With FM the full-bridge produces a symmetrical square-wave voltage and the two bride legs are operated in phase opposition. The power that flows to the load is determined by the impedance of the resonant tank and the output voltage from the

full-bridge. The FM control is usually divided into three modes which are defined as:

- **Mode I** $f_s < \frac{1}{2} f_0$
- **Mode II** $\frac{1}{2} f_0 < f_s < f_0$
- **Mode III** $f_s > f_0$

In Mode III, a higher f_s does that the impedance of the resonant tank increases and thus, a lower current, i_L, flows through the resonant tank. In this chapter, FM in Mode III is used as the primary control method.

When using FM above the resonant frequency, zero voltage switching (ZVS) at turn-ON is utilized, but there is a hard turn-OFF. A snubber capacitor, C_{SN}, in parallel with the switch and anti-parallel diode will, however, make ZVS possible at turn-OFF [**?**]. When using a capacitive snubber across a switch, it is important that the snubber capacitance is fully discharged before turning the device on in order to prevent that the remaining energy in the snubber is dissipated in the switch (snubber shoot-through).

Figure 4.2 illustrates the typical waveforms of the SLR converter. The soft flanks of the voltage transients across the high-side BJT in half-bridge leg A (AH) is seen as well as the inductor current, i_L. The pink trace shows the current of both the low-side anti-parallel Schottky diode in half-bridge leg A (AL) as well as half of the total snubber capacitance. The purple shows the current of the SiC BJT (AH). It can be seen that the BJT only conducts a majority of the current in the forward direction.

4.2 Analysis of Losses in the Full-Bridge

In this chapter, the losses of the SiC switches in the full-bridge inverter have been analyzed, and to an extent the driver consumption of the SiC BJT base driver. The losses of the complete SLR converter have not been investigated.

The losses of the devices in the full-bridge inverter can be divided into two parts: Conduction losses and switching losses.

Conduction losses

The conduction losses are subdivided into two parts for the MOSFET, and three parts for the BJT.

- The conduction losses from the BJT and MOSFET, $P_{CON,S}$.

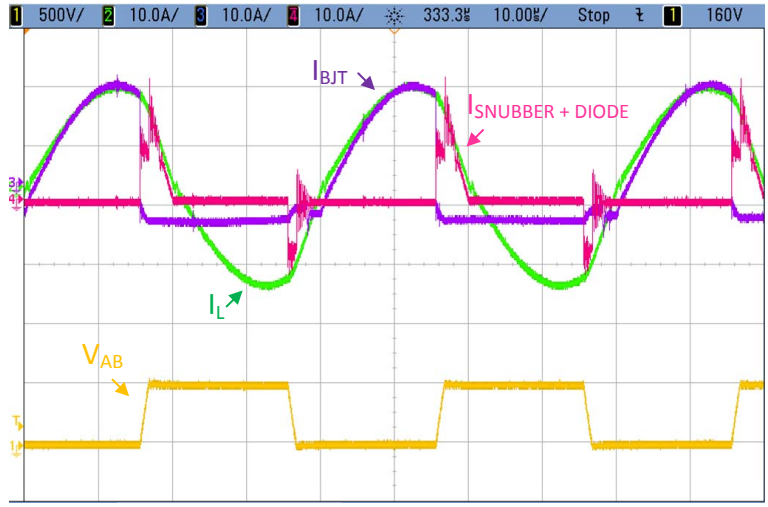

Figure 4.2: Typical waveforms for a soft-switching SLR converter populated with SiC BJTs and Schottky-diode. Currents (10 A/div), voltage (10 V/div), and time 10 (us/div)

- The conduction losses, $P_{CON,D}$, for the anti-parallel Schottky diode (in the BJT case) or body diode (in the MOSFET case).
- For the BJT, P_{BE}, mentioned in the previous chapter, also has to be considered.

$P_{CON,S}$ is defined as:

$$P_{CON,S} = \frac{1}{T_S} \int^{t_{ON}} i^2(t) \cdot R_{ON} dt, \tag{4.2}$$

where t_{ON} is the time when device is conducting the current. For the BJT also the criterion $i(t) > -I_B \cdot \beta_R$ should also be met. This means that the reverse current through the device is larger than the base current times the reverse gain, and a very small current flows through the diode. R_{ON} is the ON-state resistance of the device.

$P_{CON,D}$ is then defined as:

$$P_{CON,D} = \frac{1}{T_S} \int^{t_D} i_F(t) \cdot v_F(t) dt, \tag{4.3}$$

where t_D is the duration when the Schottky diode or body diode is conducting. The quantities $i_F(t)$ and $v_F(t)$ are the current through the device and voltage across the device respectively.

P_{BE} is then defined as

$$P_{BE} = \frac{t_{ON} \cdot I_B \cdot V_{BE}}{T_S}, \tag{4.4}$$

as has been explained previously.

The equations presented here are the losses per switch position.

Switching losses

Since ZVS is enabled during turn-ON only the turn-OFF losses are considered as switching losses.

If hard switching is employed the switching losses can be measured from the data as the integral of the product of the current and voltage during the transition time as,

$$P_{SW} = f_s \cdot E_{OFF} = f_s \cdot \int_0^{t_{OFF}} i(t) \cdot v(t) dt, \tag{4.5}$$

where E_{OFF} is the switching loss energy during turn-OFF, and t_{OFF} is the duration of the turn-OFF transient.

In the case when capacitive snubbers are used the definition of switching losses is more complicated. In this thesis it is defined as the losses that occur from the time the conducting device turns-OFF until the current starts flowing in the opposite switch position, and the losses which are associated with this process. For example, when the lower device is conducting and via the capacitive snubber the current is transitioned to the upper diode.

Figure 4.3 shows the ZVS turn-OFF process for a SiC MOSFET power module with a 400 nF capacitive snubber across. A schematic diagram of the circuit can be seen in Fig. 4.4. It can be seen that the switching loss has two major contributions. First, the duration when the MOSFET is turning off and the current, i_2, goes from the turn-OFF magnitude of the current, I_{OFF} to 0 A. It can be seen in Fig. 4.3 that the voltage increases during this period. This means that (4.5) is applicable here as well to calculate the switching losses. The voltage is lower during this transient than if hard-switching would have been used. The voltage across T_2 is greater than V_{DS}. V_{DS} is measured on the module and not directly on the chip. To be able to make a proper loss analysis the voltage has to be measured directly on the chip.

The second contribution is the one discussed in [67]. The losses originate from the energy that is stored in the inductance in the loop formed by the snubber and the diode. This energy is dissipated in the circuit as the snubber current, i_{SN}, oscillates. It can be seen that the length of the period is approximately 850 ns, and with a 400 nF snubber gives a parasitic inductance of approximately 45 nH.

Two publications, [67] and [68], discuss the impact from the parasitic inductance in the transition loop when the current commutates from the capacitive snubber

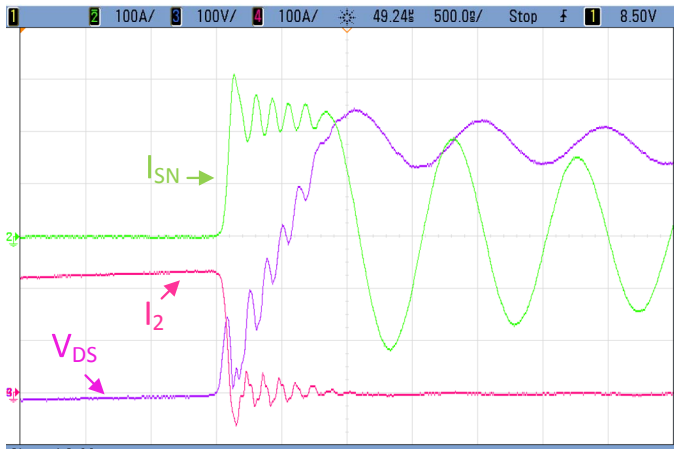

Figure 4.3: Soft-switching turn-OFF process of CREE SiC MOSFET power module with 400 nF snubber. Currents (100 A/div), voltage (100 V/div), and time 500 (ns/div)

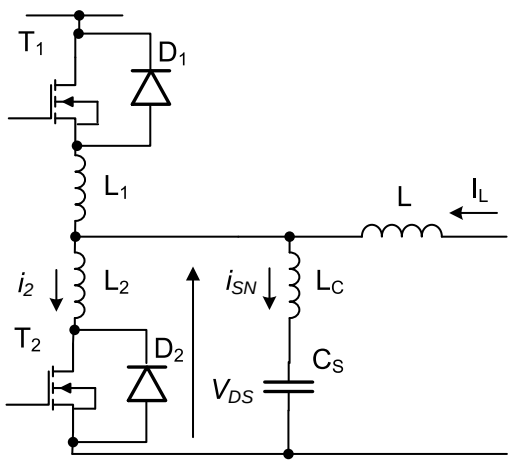

Figure 4.4: Half-bridge circuit related to the turn-OFF procedure seen in Fig. 4.3.

to the diode. Another publication, [69], thoroughly explains the impact of the capacitive snubber during the turn-OFF transients of Si IGBTs. What neither of these publications discuss is the impact of parasitic inductance during the turn-OFF of the device.

These two loss components are the major contributors to the total switching

loss. There are also some minor contributions, such as:

- P_{SB} as mentioned in Section 3.2 and (3.2).
- There are also some minor losses from the oscillation between the capacitive snubber and the parasitic capacitance of the SiC devices. These oscillations can be seen in Fig. 4.3 during the charging time of the capacitive snubber.

4.3 Experimental setup

In order to evaluate the losses for the different aspects being tested, a 6 kW test system was designed, Fig. 4.5. It is an LCC-resonant converter with the resonant inductance, L_{RES}, in series with the resonant capacitor, C_{RES}, and a capacitance, C_W, in parallel with the load. In the setup, C_W is located at the input of the diode rectifier bridge. As described in [70,71], C_W adds to the stability and controllability when using FM, especially at high load voltages. C_W is chosen to be approximately 10 % of C_{RES}. Photographs of the setup can be seen in Fig. 4.6a and Fig. 4.6b.

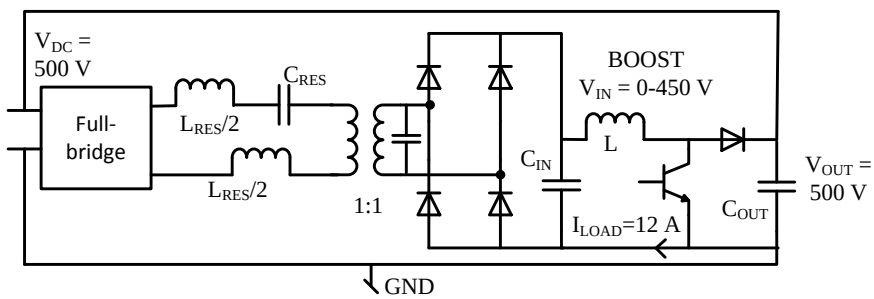

Figure 4.5: Schematics of experimental test setup.

The output from the resonant tank is isolated via a 1:1 transformer and then rectified by diodes. Since V_{DC} is constant, the load voltage, V_{LOAD}, is varied by a boost-converter. V_{LOAD} in this setup is the same as the input voltage, V_{IN}, of the boost converter. Thus,

$$V_{LOAD} = V_{DC}(1 - D), \tag{4.6}$$

where D is the duty-ratio of the boost-converter. The switching frequency of the boost-converter is 30 kHz. For all measurement points I_{LOAD} is constant but V_{LOAD} is measured in intervals from 0 % - 90 % of V_{DC}. The parameters of the system can be seen in Table 4.1. I_{LOAD} is measured by means of a shunt resistor

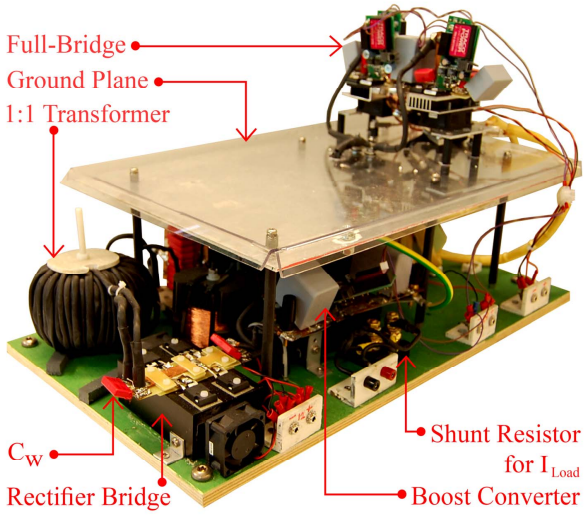

(a)

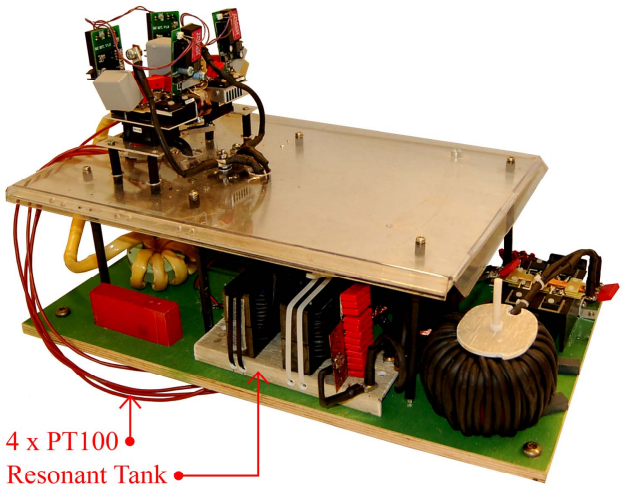

(b)

Figure 4.6: Photograph of the (a) front side and (b) backside of the experimental setup.

as seen in Fig. 4.6a. Three different resonant tanks are used during the testing with increasing resonant frequency.

Table 4.1: Parameters and variables of the experimental setup.

V_{DC}	I_{LOAD}	V_{LOAD}	C_{IN}	C_{OUT}	C_{DCL}
500 V	12 A	0-450 V	10 μF	20 μF	30 μF
Resonant	L_{RES}	C_{RES}	C_W	C_{SN}	f_S
Tank 1	348.8 μH	180 nF	15 nF	10, 20, 40 nF	24.9-28.2 kHz
Resonant	L_{RES}	C_{RES}	C_W	C_{SN}	f_S
Tank 2	90.7 μH	45 nF	4.4 nF	4.4, 8.8 nF	98-111 kHz
Resonant	L_{RES}	C_{RES}	C_W	C_{SN}	f_S
Tank 3	50 μH	25 nF	2.2 nF	4.4 nF	182-198 kHz

Device under test

Two different devices, a MOSFET without any additional anti-parallel diode and a BJT with an added anti-parallel Schottky diode, are tested in the full-bridges as seen in Fig. 4.7. The device parameters are given in Table 4.2. In all the test except one the snubber capacitance is divided equally between the upper and lower switch positions. With *Resonant Tank 1* and a C_{SN} of 10 nF, the full capacitance is over the lower switch. Three different designs are used on the full bridge:

- For FM, the full-bridge is utilizing capacitive snubbers on both half-bridge legs.
- FM is also tested with hard switching, meaning that no capacitive snubbers are utilized.
- for DuC, leg B has snubbers and leg A has no snubbers.

Only one design, with snubbers across all switch positions, is illustrated in Fig. 4.7.

Table 4.2: 1200 V SiC devices under test

Device	**SiC MOSFET**	**SiC BJT**	**SiC Schottky-diode**
Voltage rating $[V]$	1200	1200	1200
Current rating $[A]$	50	50	30 @ 145 $°C$
R_{ON} $[m\Omega]$	25	17	-
Forward voltage $[V]$	-	-	1.8 @ 30A

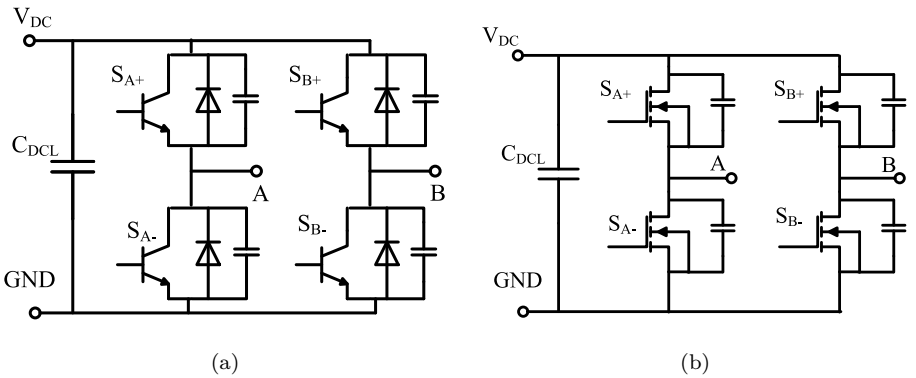

(a) (b)

Figure 4.7: Full-bridge for experimental setup with capacitive snubbers. a) are MOSFETs without anti-parallel diodes and b) BJTs with diodes.

Gate and Base Drivers

The BJT is controlled by the 2SRC driver presented by Rabkowski et al., [**Publication III**], with a V_{CCL} of 5 V and a V_{CCH} of 24 V, a base resistance, R_B, of 2.35 Ω, a depletion resistance, R_{DP}, of 1.0 Ω and a base capacitor, C_B, of 32 nF. The MOSFET is controlled by a simple totem-pole driver with +24 V/-10 V, a turn-ON gate resistance, R_{ON}, of 20 Ω and a turn-OFF gate resistance, R_{OFF}, of 30 Ω. The schematic diagrams of the drivers are seen in Fig. 4.8.

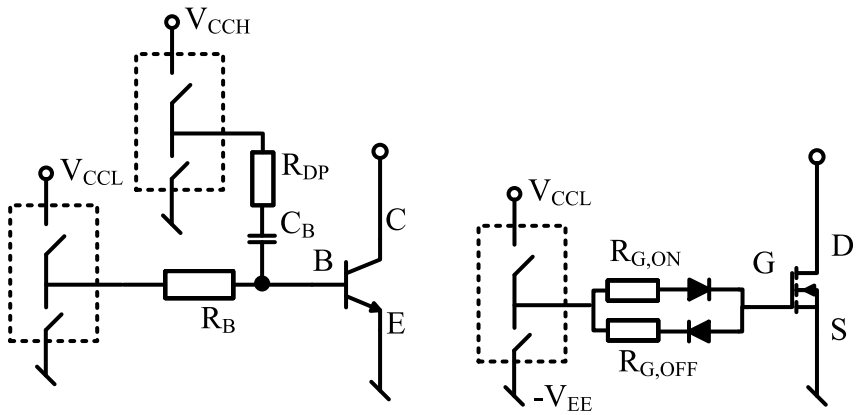

(a) (b)

Figure 4.8: Simplified schematics of a) base driver and b) gate driver.

Power loss measurement

A direct measurement of input and output voltages and currents to measure the power loss over the full-bridge is efficient, but not accurate due to the high bandwidth of the signals. In addition, the gate and base drivers generate losses in the device which are not included in the input and output powers of the full-bridge. A calorimetric method has been developed to measure the losses of the full-bridge more accurately. This is done via a thermo-electric measurement which measures the input temperature of the fan on each heat-sink, $T_{amb,A}$ and $T_{amb,B}$, and the temperatures of the heat-sinks, $T_{hs,A}$ and $T_{hs,B}$.

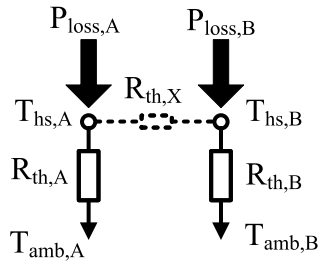

Figure 4.9: Equivalent thermal circuit.

During calibration, the thermal resistances, $R_{th,A}$ and $R_{th,B}$, from heat-sink to ambient are calculated. This is done by having a constant power for a certain time such that the temperature of the heat-sink is stabilized. Then, the power input and the temperatures are measured accurately. This is done for a certain number of power inputs such that $R_{th,A}$ and $R_{th,B}$ can be calculated.

Temperature measurements are then taken during testing and the power loss, P_{LOSS}, can be calculated with the thermal resistances, $R_{th,A}$ and $R_{th,B}$ as

$$P_{LOSS} = T_{\Delta,A} \cdot R_{th,A} + T_{\Delta,B} \cdot R_{th,B}, \tag{4.7}$$

where $T_{\Delta,A}$ and $T_{\Delta,B}$ are the differences between the ambient temperature and the temperature of the heat sink on each bridge-leg. $R_{th,X}$ represents the thermal cross-coupling between the two bridge-legs. When the total loss of the full-bridge is sought, $R_{th,X}$ is not needed. On the other hand, when the losses of each bridge shoud be determined, $R_{th,X}$ is essential. The measured total losses are estimated to have an inaccuracy of less than 5 %.

4.4 Discussion of results

This section discusses the six aspects contributing to the losses of the converter, as mentioned in the beginning of this chapter.

Load voltage

For each device, each resonant tank, each snubber value, and each control method, the losses of the full-bridge are measured at five different load voltages. The load voltage influences both the conduction and the switching losses. As the load voltage is reduced, the voltage across the resonant tank increases, and since I_{LOAD} is constant in all experiments, the frequency is increased such that the impedance increases. As the impedance increases, the resonant tank becomes more inductive. The current wave-form is then less sinusoidal and more triangular, thus increasing the RMS current. This is exemplified in Fig. 4.11 for the MOSFET full-bridge loaded with *Resonant Tank 2*. The resonant tank also becomes more inductive, meaning that the voltage leads by almost 90° at a V_{LOAD} of 0 V. This in turn, for the BJT full-bridge, forces the current through the Schottky diode for a longer duration, increasing the conduction losses. For the MOSFET full-bridge the increased duration of the body diode conducting can be eliminated with a correct dead-time control. Also, the switching losses increase with a reduced load voltage. The magnitude of the turn-OFF current, I_{OFF}, increases as well as the the switching frequency.

Device

The BJT and MOSFET are two very different devices with some similarities as discussed in Section 2.2. The main difference when a resonant converter is considered is that the MOSFET has the possibility to conduct the current in the reverse direction. This reduces the voltage drop compared to that of a Schottky diode or of the body diode. The other real differences are that the base current of the SiC BJT adds to the losses via P_{BE} and that the SiC MOSFET has a body diode that can conduct the current during the dead-time. Even though an investigation on thermal dependency has not been carried out in the scope of this thesis, it has been presented previously that the conduction losses of the SiC BJT are less dependent of the temperature compared to the SiC MOSFET [39, 49].

Switching frequency

The resonant tank is a large part of the cost in resonant converters. What SiC devices enable, due to their lower switching losses compared to Si IGBTs, is to

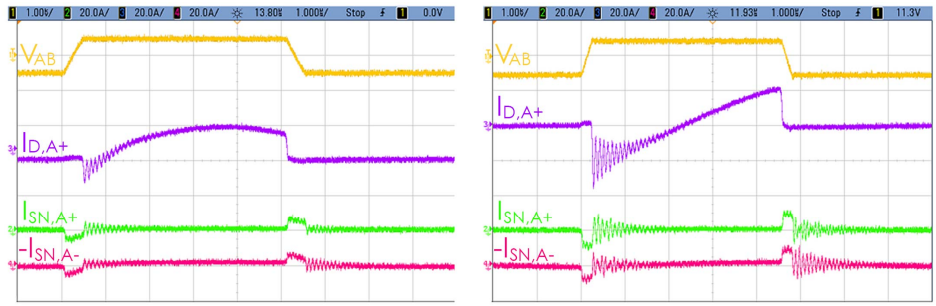

(a) (b)

Figure 4.10: Typical voltage and current curves at 90% load voltage (a) and at 0% load voltage (b). Currents (20 A/div), voltage (1 kV/div), and time 1000 (ns/div)

Figure 4.11: Typical voltage and current curves at 90% load voltage (a) and at 0% load voltage (b). Currents (20 A/div), voltage (1 kV/div), and time 1000 (ns/div)

increase the switching frequency when higher voltages and higher power is targeted. This means that the inductance and capacitance of the resonant tank can be reduced, implying smaller volumes, lower weights, and lower costs of the passive components. The possibility of using smaller passives is together with the reduced losses the main drive for introducing the SiC technology in resonant converters. In **Publication V**, **Publication VI** and **Publication VIII** it is shown that the losses are very small even at the higher switching frequencies.

Theoretically, regardless of the frequency the conduction losses should be constant if the impedance of the resonant tank is constant regardless of switching frequency. In reality, it is practically impossible to have exactly the same impedance at the three different frequencies. This is due to the fact that three different resonant tanks are used in the prototype with discrete values of capacitance as well as hand-wound inductance and a hand-wound transformer. This makes a comparison between the losses at different switching frequencies harder. Additionally, as the switching frequency increases from 25 kHz to 100 kHz, and to 195 kHz, the resolution of the control is decreased. The reduced resolution means that the body diode conducts the current for a longer time, which increases the losses. In theory the switching losses would scale linearly with the switching frequency.

Capacitive snubbers

The capacitive snubbers are used to enable ZVS at turn-OFF. The optimal value of the capacitive snubber is hard to derive. It needs to be sufficiently large such that the voltage across the switch does not reach V_{DC} during the turn-OFF of the switch current. The larger C_{SN} is, the smaller the losses. This is especially true for the Si IGBT which has a tail-current that contributes to the losses. This is explained in detail in [69] and [72]. For the SiC devices the size of C_{SN} is not believed to have such a large impact on the losses. What seems to be more of an impact is the shorter charging time of the snubber. This forces the body diode or Schottky diode to conduct for a longer time and thus increase the losses. For the MOSFET, this issue can be reduced as seen in Fig. 4.12. Here, the losses are shown for *Resonant Tank 1* and *Resonant Tank 2* with different values of snubber capacitance. In the two cases with reduced value of the snubber capacitance, the dead-times have been reduced accordingly. This makes the conduction time of the body diode equal for the two different values of snubber capacitance. No significant difference can be seen in the losses. This shows the importance of using a dead-time that correlates to the size of the capacitive snubber.

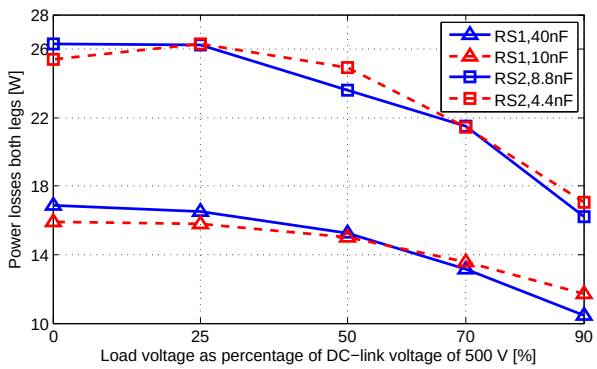

Figure 4.12: Losses in the MOSFET full-bridge when using *Resonant Tank 1* and *Resonant Tank 2* with different values of the snubber capacitance.

For the BJT on the other hand, the conduction time of the Schottky diode cannot be reduced. The losses then scale with the additional time the Schottky diode is conducting instead of the capacitive snubber. This is illustrated in Fig. 4.13, where the losses increase with a smaller capacitive snubber.

The losses for hard switching, when no capacitive snubber is added, increase more compared to the other loss curves. This is an indication of that the internal capacitances of the SiC BJT and SiC Schottky diode are not sufficient to enable

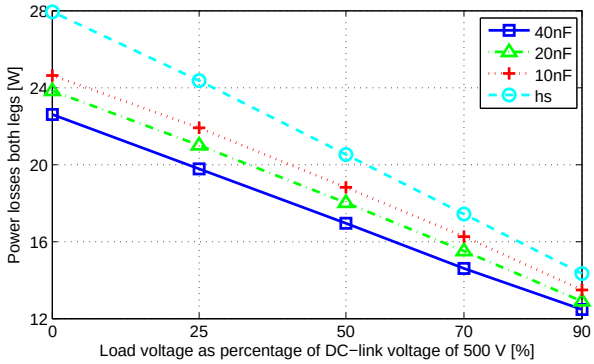

Figure 4.13: Losses in the BJT full-bridge when using *Resonant Tank 1* with different values of the snubber capacitance and hard switching.

soft-switching

Dead-time control

When using unipolar devices in resonant converters it is shown that an active control of the dead-time is important to keep the losses at a minimum over the whole range of the load voltage. This has been exemplified by comparing the losses for a SiC MOSFET using the body-diode instead of an anti-parallel diode and letting the body-diode conduct the current for different dead-times.

This is straightforward, since the shorter time the body diode conducts the higher the efficiency is. The results can be seen in Fig. 4.14. Figure 4.14 (a) shows the losses versus load-voltage when using a constant dead-time, or when using an optimized (minimized) dead-time. Figure 4.14 (b) shows the losses at 0 % load voltage for different dead-times. It is clearly shown that a minimal dead-time is preferred.

On the other hand, the losses for the full-bridge populated with SiC BJTs and anti-parallel diodes are shown experimentally to be less dependent on the dead-time. This is due to the fact that the SiC BJT cannot conduct the full current in the reverse direction. However, it is important to note that even though the losses of the full-bridge are almost independent of the dead-time, the base driver consumption for all four positions can be reduced up to 3 W by maximizing the dead-time to an optimum. This is illustrated in Fig. 4.15 where the dead-time is decreased from the maximum dead-time of 2000 ns to the minimum, 350 ns. How the driver consumption relates to the dead-time is illustrated in Fig. 4.16.

Another aspect regarding the power consumption of the base drivers is that

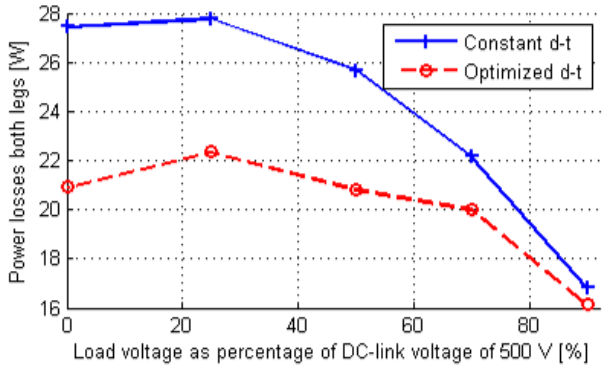

(a)

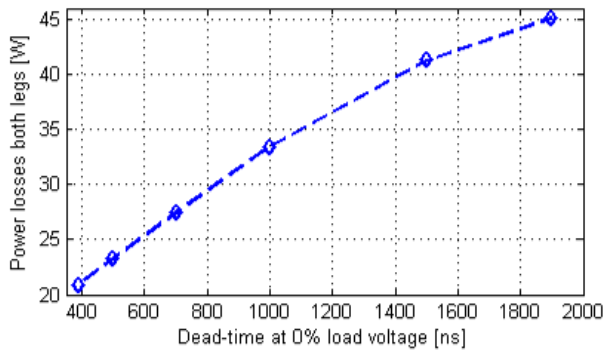

(b)

Figure 4.14: *Resonant tank 2* and MOSFET full-bridge: (a) Power loss of the MOSFET full-bridge over the full load-voltage range and (b) Power loss of the MOSFET full-bridge at 0 % load-voltage vs dead-time.

V_{BE} reduces when the SiC BJT has a reverse current. The consequence of this is an increased base current with an associated increase of the power consumption of the base driver. This was discussed in Section 3.4.

Control method

For FM the output power is controlled by simply adjusting the switching frequency of the full-bridge. The duty-ratio is 50 %. When comparing different control methods it was chosen to keep the dead-time constant over the full load voltage range, even though it has been proven that an active dead-time control can reduce the losses compared to a constant dead-time.

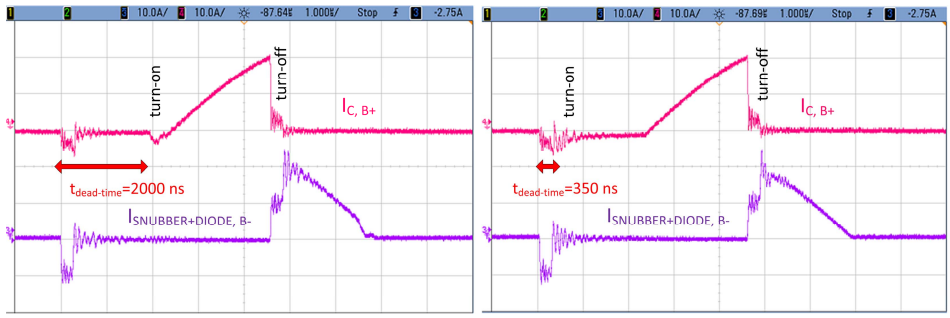

(a) (b)

Figure 4.15: Voltage and current curves to illustrate the dead-time control for BJT full-bridge at 0% load voltage. In a) $t_{dt} = 2000\ ns$ and in b) $t_{dt} = 350\ ns$.

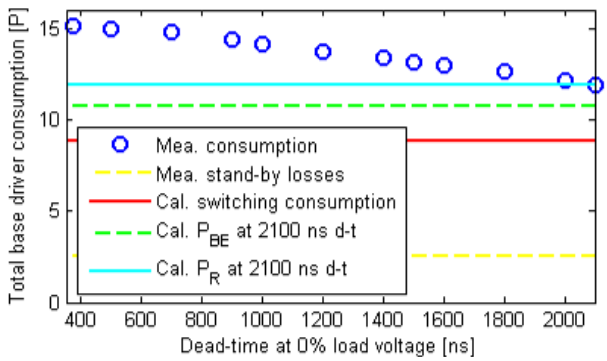

Figure 4.16: Total measured consumption of the four BJT drivers with respect to dead-time. The straight lines are from bottom: stand-by driver losses, calculated switching losses, calculated P_{BE} with a dead-time of 2100 ns and calculated P_R with a dead-time of 2100 ns. f_s is 110 kHz.

For DuC, as presented in **Publication VII**, the output power is controlled by a combination of frequency control and phase control. The goal of this control method is to have the transistors in leg A, the leg with no capacitive snubbers, to turn-OFF as late as possible before the zero-current crossing. This makes it possible for both ZVS turn-ON and close to ZCS turn-OFF of the transistors in leg A. Also, the current in these switches will almost only see positive current and very small anti-parallel diode or body-diode currents. The currents in the transistors in leg B, on the other hand, will see higher turn-OFF currents as well as longer

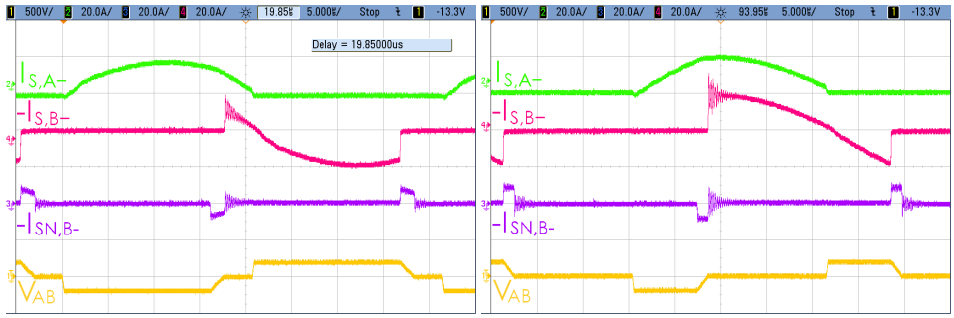

(a) (b)

Figure 4.17: DuC operation with *Resonant Tank 1* at (a) 90% and (b) 25% of load voltage. Measured current of the leg A, (top, 20 A/div), current of the leg B, (next to top, 20 A/div), snubber current on leg B (next to bottom, 20 A/div), output voltage of the full bridge, (bottom, 1 kV/div), (time-base 5 us/div).

periods of reverse conduction. The magnitude of the turn-OFF current as well as the duration of the reverse conduction during every cycle is dependent on the load voltage and load current. Figure 4.17 illustrates the operation of DuC at different load voltages.

The losses for the MOSFET full-bridge can be seen in Fig. 4.18 as a function of the load-voltage. It is seen, as the voltage over the resonant tank increases the efficiency of DuC compared to FM is improved.

For the BJT full-bridge inverter it can be seen that there is no gain in efficiency. The losses are instead distributed unevenly between the half-bridges and also between the devices per switch-position. In half-bridge leg B the dominant losses are in the Schottky diode, and in leg A in the SiC BJT. The losses in half-bridge leg B could be reduced if an active dead-time control is used instead of a constant dead-time, since the BJT can be in the OFF-state during the time the Schottky diode is forward biased.

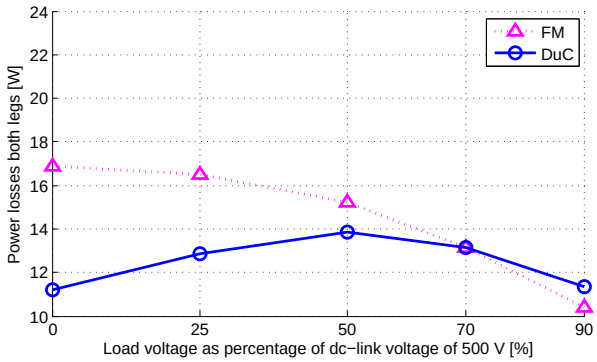

(a)

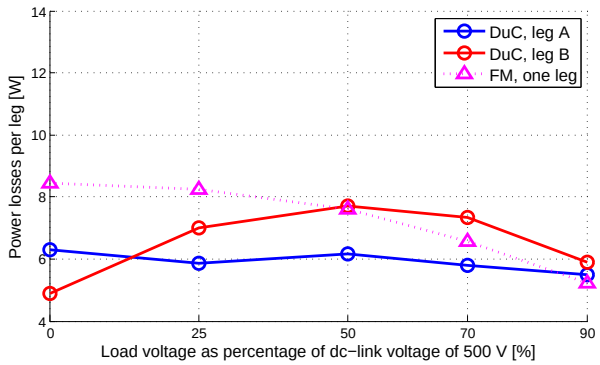

(b)

Figure 4.18: Losses in the MOSFET full-bridge when using *Resonant Tank 1* as a function of load-voltage: (a) Power loss of the MOSFET full-bridge and (b) Power loss per leg.

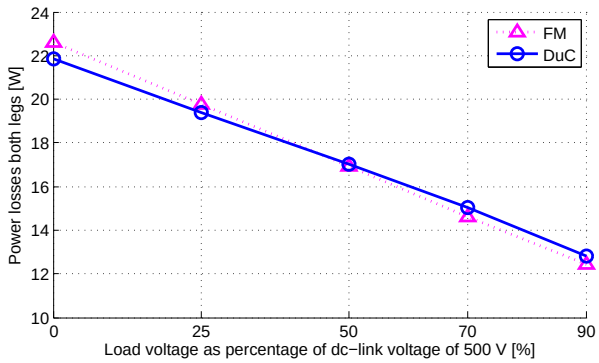

(a)

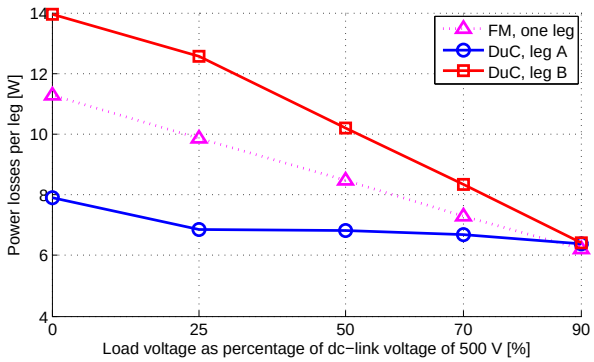

(b)

Figure 4.19: Losses in the BJT full-bridge when using *Resonant Tank 1* as a function of load-voltage: (a) Power loss of the BJT full-bridge and (b) Power loss per leg.

Chapter 5

Conclusions and Future Work

This chapter concludes the performed work presented in this thesis and proposes some future work that the author deems important.

5.1 Conclusions

In this thesis, different base driver concepts for SiC power BJTs have been presented. The consumption of the base driver is divided into smaller parts that have been analyzed. It is shown that the bipolar SiC BJT behaves like a unipolar SiC device with a low on-state voltage drop and fast switching transients. Furthermore, the 2SRC base driver is introduced which manages to switch the device below 50 ns while still keeping the base driver consumption at an acceptable level.

For applications with a variable load current, proportional base drivers could be used. This concept is introduced with a special focus on the DPBD. By implementing the DPBD concept and building a prototype it is shown that the steady-state consumption of the base driver can be reduced considerably.

The increased voltage over the base driver during reverse conduction of the SiC BJT has been discussed. Even though this issue is not as big for the SiC BJT as it was for the Si BJT, it still needs to be considered. Three solutions are proposed, and two of them are compared experimentally.

SiC devices in SLR converters are shown, not to just have lower ON-state losses, but also to reduce the switching losses substantially. This makes SiC transistors to be great candidates in order to increase the switching frequency, and thus reducing the size and cost of the passive components in the resonant tank. There are many aspects that need to be evaluated in order to really optimize the design for the SiC technology.

It is shown, especially for SiC unipolar devices, how important the optimization of the dead-time is to keep the conduction losses low.

Since the SiC device has no tail-current, the size of the capacitive snubbers can be reduced considerably without increasing the losses. What is shown to happen in this thesis is that the losses increase with smaller capacitive snubbers, especially for the BJT, but this is mostly due to the increased conduction time of the anti-parallel Schottky diode, and in a smaller part to the increased magnitude of the transition current from the capacitive snubbers to the diode. For the full-bridge populated with MOSFETs, the losses were approximately the same if the dead-time was adjusted with respect to the size of the capacitive snubber.

Dual control is shown to reduce the total converter losses, and it is shown that this control methods is very advantageous for SiC unipolar devices.

5.2 Future Work

Base drivers for SiC BJTs have been published in the literature, not just by the author of this thesis. What the author is missing is the realization of the combination between the current source driver, [62], and the PWM controlled base driver, [64]. The idea was presented by the author at *ECCE ASIA Downunder 2013* in Melbourne and is presented briefly in **Publication II**. Sadly, there was no time to dive further into this driver concept and to take it from idea to prototype. The benefits with this driver instead of the drivers presented in this thesis is that it could be a single-source solution with just two passives, a base resistor and a base inductor, and that it can follow the collector current with an infinite number of discrete levels.

For the SLR converter there are still many things that need to be considered. How important is the speed of the turn-ON and turn-OFF transients for soft-switching, and how small can the capacitive snubber be? A small comparison was made in this thesis, but not one as thorough as the author would have desired. In this thesis, the transients for the BJT were very fast, but the transients for the MOSFET were slower. This could be seen on the losses, especially at higher switching frequencies and hard switching.

Even though experimental testing was carried out to see that the losses increased when an additional inductance was added in the snubber loop, [68], a more thorough theoretical and experimental analysis should be done to clearly investigate the impact from the parasitic inductance in the snubber loop.

All the work done for the SLR converter should make it possible to deliver a full-bridge resonant LCC converter in the range of 20 kW - 100 kW with switching frequencies above 500 kHz, with a considerably higher efficiency than today's tech-

nologies, i.e. Si IGBTs. With an optimized SiC module with integrated snubbers and driver parts even higher frequencies, or powers, should be reachable.

List of Acronyms

2SRC dual-source

AC or ac alternating current

BJT bipolar junction transistor

DC or dc direct current

DSP digital signal processor

DPBD discretized proportional base driver

DuC dual control

EV electric vehicle

FM frequency modulation

GaN gallium nitride

HEV hybrid electric vehicle

HVDC high voltage direct current.

IGBT insulated-gate bipolar transistor

JFET junction field-effect transistor

LCVJFET lateral channel vertical junction field-effect transistor

M2C modular multilevel converter

MOSFET metal-oxide semiconductor field-effect transistor

NEDC New European Driving Cycle

PM phase modulation

PV	photo voltaic
PWM	pulse-width modulated
Si	silicon
SiC	silicon carbide
SLR	series-loaded resonant
WBG	wide band-gap
ZCS	zero current switching
ZVS	zero voltage switching

Bibliography

[1] L. Day and I. McNeil, *Biographical dictionary of the history of technology.* London: London: Routledge, 1966.

[2] T. J. Price, *Oxford Dictionary of National Biography.* Oxford: Oxford University Press, 2004.

[3] G. Asplund, K. Eriksson, and K. Svensson, "DC transmission based on voltage source converters," in *CIGRE SC14 Colloquium in South Africa 1997*, 1997.

[4] B. Ozpineci and L. Tolbert, "Smaller, faster, tougher," *Spectrum, IEEE*, vol. 48, no. 10, pp. 45–66, October 2011.

[5] J. Rabkowski, D. Peftitsis, and H.-P. Nee, "Silicon carbide power transistors: A new era in power electronics is initiated," *Industrial Electronics Magazine, IEEE*, vol. 6, no. 2, pp. 17–26, June 2012.

[6] U. Lamm, "Mercury-arc valves for high voltage dc transmission," *IEE Proceedings*, vol. 3, no. 10, pp. 1747–1753, 1964.

[7] W. Shockley, "A unipolar "field-effect" transistor," *Proceedings of the IRE*, vol. 40, no. 11, pp. 1365–1376, Nov 1952.

[8] R. Prest and J. Van Wyk, "Reverse bipolar transistor conduction in high-current pwm inverters," *Power Electronics, IEEE Transactions on*, vol. 3, no. 3, pp. 246–253, July 1988.

[9] S. Hofstein and F. Heiman, "The silicon insulated-gate field-effect transistor," *Proceedings of the IEEE*, vol. 51, no. 9, pp. 1190–1202, Sep. 1963.

[10] H. Becke and C. Wheatley Jr, "Power MOSFET with an anode region," United States of America Patent 4,364,073, December 14, 1982.

[11] B. Baliga, M. Adler, P. Gray, R. Love, and N. Zommer, "The insulated gate rectifier (IGR): A new power switching device," in *Proceedings of the 1982 International Electron Devices Meeting*, vol. 28, 1982, pp. 264–267.

[12] A. Lidow, J. Strydom, R. Strittmatter, and C. Zhou, "Gan: A reliable future in power conversion: Dramatic performance improvements at a lower cost," *Power Electronics Magazine, IEEE*, vol. 2, no. 1, pp. 20–26, March 2015.

[13] K. Bergman, "Silicon carbide - the power semiconductor material of the future," *ABB Review*, no. 1, pp. 37–42, 1996.

[14] H. Lendenmann, A. Mukhitdinov, F. Dahlqvist, H. Bleichner, M. Irwin, and R. Söderholm, "4.5 kV 4H-SiC diodes with ideal forward characteristic," in *Proceedings of the 13th International Symposium on Power Semiconductor Devices and ICs, 2001, ISPSD '01*, 2001, pp. 31–34.

[15] W. Vetter, J. Liu, M. Dudley, M. Skowronski, H. Lendenmann, and C. Hallin, "Dislocation loops formed during the degradation of forward-biased 4H–SiC p-n junctions," *Materials Science and Engineering*, vol. B98, pp. 220–224, 2003.

[16] J. Palmour, "Silicon carbide power device development for industrial markets," in *Electron Devices Meeting (IEDM), 2014 IEEE International*, Dec 2014, pp. 1.1.1–1.1.8.

[17] P. Friedrichs, H. Mitlehner, R. Schörner, K.-O. Dohnke, R. Elpelt, and D. Stephani, "The vertical silicon carbide JFET – a fast and low loss solid state power switching device," in *Proceedings of the 9th European Conference on Power Electronics and Applications, EPE'01, Graz*, 2001, pp. 1–6.

[18] H. Mitlehner, W. Bartsch, K. Dohnke, P. Friedrichs, R. Kaltschmidt, U. Weinert, B. Weis, and D. Stephani, "Dynamic characteristics of high voltage 4H-SiC vertical JFETs," in *Proceedings of the 11th International Symposium on Power Semiconductor Devices and ICs, 1999, ISPSD '99*, 1999, pp. 339–342.

[19] M. Bhatnagar, P. McLarty, and B. Baliga, "Silicon-carbide high-voltage (400 V) schottky barrier diodes," *IEEE Electron Device Letters*, vol. 13, no. 10, pp. 501–503, Oct. 1992.

[20] R. Wang, Z. Chen, D. Boroyevich, L. Jiang, Y. Yao, and K. Rajashekara, "A novel hybrid packaging structure for high-temperature sic power modules," *Industry Applications, IEEE Transactions on*, vol. 49, no. 4, pp. 1609–1618, July 2013.

[21] C. Weitzel, J. Palmour, J. Carter, C.H., K. Moore, K. J. Nordquist, S. Allen, C. Thero, and M. Bhatnagar, "Silicon carbide high-power devices," *Electron Devices, IEEE Transactions on*, vol. 43, no. 10, pp. 1732–1741, Oct 1996.

[22] M. Bhatnagar and B. Baliga, "Comparison of 6h-sic, 3c-sic, and si for power devices," *Electron Devices, IEEE Transactions on*, vol. 40, no. 3, pp. 645–655, Mar 1993.

[23] Z. Chen, Y. Yao, D. Boroyevich, K. Ngo, P. Mattavelli, and K. Rajashekara, "A 1200-v, 60-a sic mosfet multichip phase-leg module for high-temperature, high-frequency applications," *Power Electronics, IEEE Transactions on*, vol. 29, no. 5, pp. 2307–2320, May 2014.

[24] R. Khazaka, l. Mendizabal, D. Henry, and R. Hanna, "Survey of high-temperature reliability of power electronics packaging components," *Power Electronics, IEEE Transactions on*, vol. 30, no. 5, pp. 2456–2464, May 2015.

[25] J. Rabkowski, D. Peftitsis, and H.-P. Nee, "Parallel-operation of discrete sic bjts in a 6-kw 250-khz dc-dc boost converter," *Power Electronics, IEEE Transactions on*, vol. 29, no. 5, pp. 2482–2491, May 2014.

[26] A. Anthon, Z. Zhang, and M. Andersen, "A high power boost converter for pv systems operating up to 300 khz using sic devices," in *Electronics and Application Conference and Exposition (PEAC), 2014 International*, Nov 2014, pp. 302–307.

[27] J. Rabkowski, D. Peftitsis, and H.-P. Nee, "Design steps toward a 40-kva sic jfet inverter with natural-convection cooling and an efficiency exceeding 99.5 %," *Industry Applications, IEEE Transactions on*, vol. 49, no. 4, pp. 1589–1598, July 2013.

[28] J. Colmenares, D. Peftitsis, G. Tolstoy, D. Sadik, H.-P. Nee, and J. Rabkowski, "High-efficiency three-phase inverter with sic mosfet power modules for motor-drive applications," in *Energy Conversion Congress and Exposition (ECCE), 2014 IEEE*, Sept 2014, pp. 468–474.

[29] M. Kamikura, Y. Murata, T. Kutsuki, and K. Saito, "Application trend and foresight of sic power devices to air conditioners," in *Power Electronics Conference (IPEC-Hiroshima 2014 - ECCE-ASIA), 2014 International*, May 2014, pp. 2064–2067.

[30] H. Wang, O. Ikawa, S. Miyashita, T. Nishimura, and S. Igarashi, "1700v si-igbt and sic-sbd hybrid module for ac690v inverter system," in *Power Electronics Conference (IPEC-Hiroshima 2014 - ECCE-ASIA), 2014 International*, May 2014, pp. 3702–3706.

[31] K. Ishikawa, K. Ogawa, S. Yukutake, N. Kameshiro, and Y. Kono, "Traction inverter that applies compact 3.3 kv / 1200 a sic hybrid module," in *Power*

Electronics Conference (IPEC-Hiroshima 2014 - ECCE-ASIA), 2014 International, May 2014, pp. 2140–2144.

[32] A. Tripathi, K. Hatua, K. Mainali, D. Patel, A. Kadavelugu, S. Hazra, and S. Bhattacharya, "Design considerations of a 15kv sic igbt based medium-voltage high-frequency isolated dc-dc converter," *Industry Applications, IEEE Transactions on*, vol. PP, no. 99, pp. 1–1, 2015.

[33] S. Madhusoodhanan, K. Hatua, S. Bhattacharya, S. Leslie, S.-H. Ryu, M. Das, A. Agarwal, and D. Grider, "Comparison study of 12kv n-type sic igbt with 10kv sic mosfet and 6.5kv si igbt based on 3l-npc vsc applications," in *Energy Conversion Congress and Exposition (ECCE), 2012 IEEE*, Sept 2012, pp. 310–317.

[34] S. Safari, A. Castellazzi, and P. Wheeler, "Experimental and analytical performance evaluation of sic power devices in the matrix converter," *Power Electronics, IEEE Transactions on*, vol. 29, no. 5, pp. 2584–2596, May 2014.

[35] R. Callanan, J. Rice, and J. Palmour, "Third quadrant behavior of sic mosfets," in *Applied Power Electronics Conference and Exposition (APEC), 2013 Twenty-Eighth Annual IEEE*, March 2013, pp. 1250–1253.

[36] D. Peftitsis, J. Rabkowski, and H.-P. Nee, "Self-powered gate driver for normally on silicon carbide junction field-effect transistors without external power supply," *Power Electronics, IEEE Transactions on*, vol. 28, no. 3, pp. 1488–1501, March 2013.

[37] D. Aggeler, F. Canales, J. Biela, and J. Kolar, "D v /d t -control methods for the sic jfet/si mosfet cascode," *Power Electronics, IEEE Transactions on*, vol. 28, no. 8, pp. 4074–4082, Aug 2013.

[38] D.-P. Sadik, J. Colmenares, D. Peftitsis, J.-K. Lim, J. Rabkowski, and H.-P. Nee, "Experimental investigations of static and transient current sharing of parallel-connected silicon carbide mosfets," in *Power Electronics and Applications (EPE), 2013 15th European Conference on*, Sept 2013, pp. 1–10.

[39] P. Ranstad, H.-P. Nee, J. Linner, and D. Peftitsis, "An experimental evaluation of sic switches in soft-switching converters," *Power Electronics, IEEE Transactions on*, vol. 29, no. 5, pp. 2527–2538, May 2014.

[40] Z. Zhang, F. Wang, L. Tolbert, and B. Blalock, "Active gate driver for crosstalk suppression of sic devices in a phase-leg configuration," *Power Electronics, IEEE Transactions on*, vol. 29, no. 4, pp. 1986–1997, April 2014.

[41] J. Colmenares, D. Peftitsis, J. Rabkowski, D.-P. Sadik, and H.-P. Nee, "Dual-function gate driver for a power module with sic junction field-effect transistors," *Power Electronics, IEEE Transactions on*, vol. 29, no. 5, pp. 2367–2379, May 2014.

[42] D.-P. Sadik, J. Colmenares, D. Peftitsis, G. Tolstoy, J. Rabkowski, and H.-P. Nee, "Analysis of short-circuit conditions for silicon carbide power transistors and suggestions for protection," in *Power Electronics and Applications (EPE'14-ECCE Europe), 2014 16th European Conference on*, Aug 2014, pp. 1–10.

[43] A. Agarwal, M. Das, B. Hull, S. Krishnaswami, J. Palmour, J. Richmond, S.-H. Ryu, and J. Zhang, "Progress in silicon carbide power devices," in *Device Research Conference, 2006 64th*, June 2006, pp. 155–158.

[44] S. Sundaresan, S. Jeliazkov, B. Grummel, and R. Singh, "10 kv sic bjts static, switching and reliability characteristics," in *Power Semiconductor Devices and ICs (ISPSD), 2013 25th International Symposium on*, May 2013, pp. 303–306.

[45] H. Elahipanah, A. Salemi, C.-M. Zetterling, and M. Östling, "5.8-kv implantation-free 4h-sic bjt with multiple-shallow-trench junction termination extension," *Electron Device Letters, IEEE*, vol. 36, no. 2, pp. 168–170, Feb 2015.

[46] A. Lindgren and M. Domeij, "Degradation free fast switching 1200 v 50 a silicon carbide bjt's," in *Applied Power Electronics Conference and Exposition (APEC), 2011 Twenty-Sixth Annual IEEE*, March 2011, pp. 1064–1070.

[47] H. Zhang, L. Tolbert, and B. Ozpineci, "Impact of sic devices on hybrid electric and plug-in hybrid electric vehicles," *Industry Applications, IEEE Transactions on*, vol. 47, no. 2, pp. 912–921, March 2011.

[48] L. Breazeale and R. Ayyanar, "A photovoltaic array transformer-less inverter with film capacitors and silicon carbide transistors," *Power Electronics, IEEE Transactions on*, vol. 30, no. 3, pp. 1297–1305, March 2015.

[49] H. Sarnago, O. Lucia Gil, and J. Burdio, "A comparative evaluation of sic power devices for high performance domestic induction heating," *Industrial Electronics, IEEE Transactions on*, vol. PP, no. 99, pp. 1–1, 2015.

[50] V. Esteve, J. Jordan, E. Sanchis-Kilders, E. Dede, E. Maset, J. Ejea, and A. Ferreres, "Comparative study of a single inverter bridge for dual-frequency induction heating using si and sic mosfets," *Industrial Electronics, IEEE Transactions on*, vol. 62, no. 3, pp. 1440–1450, March 2015.

[51] S. Allebrod, R. Hamerski, and R. Marquardt, "New transformerless, scalable modular multilevel converters for hvdc-transmission," in *Power Electronics Specialists Conference, 2008. PESC 2008. IEEE*, June 2008, pp. 174–179.

[52] H. van der Broeck, J. van Wyk, and J. Schoeman, "On the steady-state and dynamic characteristics of bipolar transistor power switches in low-loss technology," *Electric Power Applications, IEE Proceedings B*, vol. 132, no. 5, pp. 251–259, September 1985.

[53] A. Lindgren and M. Domeij, "Fast switching 1200 v 50 a silicon carbide bjt's in boost converters," in *Power Electronics and Applications (EPE 2011), Proceedings of the 2011-14th European Conference on*, Aug 2011, pp. 1–8.

[54] S. Sundaresan, A.-M. Soe, S. Jeliazkov, and R. Singh, "Characterization of the stability of current gain and avalanche-mode operation of 4h-sic bjts," *Electron Devices, IEEE Transactions on*, vol. 59, no. 10, pp. 2795–2802, Oct 2012.

[55] *datasheet CAS300M12BM2*, CREE Inc., 2014, rev. -.

[56] B. Ållebrand, "On sic jfet converters: components, gate-drives and main-circuit conditions," Ph.D. dissertation, KTH, Electrical Machines and Power Electronics (closed 20110930), 2005.

[57] D. Peftitsis, J. Rabkowski, G. Tolstoy, and H. Nee, "Experimental comparison of dc-dc boost converters with sic jfets and sic bipolar transistors," in *Power Electronics and Applications (EPE 2011), Proceedings of the 2011-14th European Conference on*, Aug 2011, pp. 1–9.

[58] R. Prest and J. Van Wyk, "Pulsed transformer base drives for high-efficiency high-current low-voltage switches," *Power Electronics, IEEE Transactions on*, vol. 3, no. 2, pp. 137–146, April 1988.

[59] J. Enslin and S. Hartman, "A novel isolated, compensated darlington based-drive configuration," in *Industry Applications Society Annual Meeting, 1991., Conference Record of the 1991 IEEE*, Sept 1991, pp. 939–945 vol.1.

[60] J. Joyce and J. Kress, "Power transistor switching with a controlled regenerative current mode transformer," in *Power Electronics Specialists Conference, 1977 IEEE*, June 1977, pp. 148–155.

[61] R. Kelley, A. Ritenour, D. Sheridan, and J. Casady, "Improved two-stage dc-coupled gate driver for enhancement-mode sic jfet," in *Applied Power Electronics Conference and Exposition (APEC), 2010 Twenty-Fifth Annual IEEE*, Feb 2010, pp. 1838–1841.

[62] J. Rabkowski, D. Peftitsis, H.-P. Nee, and M. Zdanowski, "A simple high-performance low-loss current-source driver for sic bipolar transistors," in *Power Electronics and Motion Control Conference (IPEMC), 2012 7th International*, vol. 1, June 2012, pp. 222–228.

[63] G. Tolstoy, D. Peftitsis, J. Rabkowski, H.-P. Nee, and P. Palmer, "A discretized proportional base driver for silicon carbide bipolar junction transistors," in *ECCE Asia Downunder (ECCE Asia), 2013 IEEE*, June 2013, pp. 728–735.

[64] H. Sarnago, O. Lucia, A. Mediano, and J. Burdio, "Improved operation of sic bjt-based series resonant inverter with optimized base drive," *Power Electronics, IEEE Transactions on*, vol. 29, no. 10, pp. 5097–5101, Oct 2014.

[65] *FSICBH017A120 Preliminary datasheet*, Fairchild Semiconductors, 2012, rev. -.

[66] P. Ranstad, H.-P. Nee, and J. Linner, "A novel control strategy applied to the series loaded resonant converter," in *Power Electronics and Applications, 2005 European Conference on*, 2005, pp. 10 pp.–P.10.

[67] P. Ranstad and J. Linner, "Aspects on sic switches for soft-switching converters in an industrial application," *ECS Transactions*, vol. 50, no. 3, pp. 75–83, 2013.

[68] P. Ranstad, F. Giezendanner, M. Bakowski, J.-K. Lim, G. Tolstoy, and A. Ranstad, "Sic power devices in a soft switching converter, including aspects on packaging," *ECS Transactions*, vol. 64, no. 7, pp. 51–59, 2014.

[69] H. Sarnago, O. Lucia, A. Mediano, and J. Burdio, "Analytical model of the half-bridge series resonant inverter for improved power conversion efficiency and performance," *Power Electronics, IEEE Transactions on*, vol. 30, no. 8, pp. 4128–4143, Aug 2015.

[70] G. Demetriades, P. Ranstad, and C. Sadarangari, "Three elements resonant converter: the lcc topology by using matlab," in *Power Electronics Specialists Conference, 2000. PESC 00. 2000 IEEE 31st Annual*, vol. 2, 2000, pp. 1077–1083 vol.2.

[71] P. Ranstad and H.-P. Nee, "On the distribution of ac and dc winding capacitances in high-frequency power transformers with rectifier loads," *Industrial Electronics, IEEE Transactions on*, vol. 58, no. 5, pp. 1789–1798, May 2011.

[72] P. Ranstad, "Control and design aspects of components and systems in high-voltage converters for industrial applications," Ph.D. dissertation, KTH, Electrical Machines and Power Electronics, 2010, qC 20101014.

Publication I

Performance tests of $4.1x4.1mm^2$ SiC JFETs for a DC/DC boost converter application

G. Tolstoy, D. Peftitsis, J. Rabkowski and H.–P. Nee

Published *in Proc. of* 8^{th} *European Conference on Silicon Carbide and Related Materials 2010*, ECSCRM 2010, pp. 722–725, 29 Aug.–2 Sept. 2010.

©2010 Reprinted with permission from AAAS.

Publication II

High-power modular multilevel converters with SiC JFETs

D. Peftitsis, **G. Tolstoy**, A. Antonopoulos, J. Rabkowski, J.–K. Lim, M. Bakowski, L. Ängquist, and H.–P. Nee

Published in *IEEE Transactions on Power Electronics*, vol.27, no.1, pp.28–36, Jan. 2012

©2012 IEEE. Reprinted with permission.

Publication III

Low-Loss High-Performance Base-Drive Unit for SiC BJTs

J. Rabkowski, **G. Tolstoy**, D. Petitsis, and H.-P. Nee

Published in *IEEE Transactions on Power Electronics*, vol.27, no.5, pp.2633–2643, May 2012

©2012 IEEE. Reprinted with permission.

Publication IV

A Discretized Proportional Base Driver for Silicon Carbide Bipolar Junction Transistors

G. Tolstoy, D. Petitsis, J. Rabkowski, P. R. Palmer, and H.-P. Nee

Published in *IEEE Transactions on Power Electronics*, vol.29, no.5, pp.2408–2617, May 2014

©2014 IEEE. Reprinted with permission.

Publication V

An experimental analysis on how the dead-time of SiC BJT and SiC MOSFET impacts the losses in a high-frequency resonant converter

G. Tolstoy, P. Ranstad, Juan Colmenares, D. Peftitsis, F. Giezendanner, J. Rabkowski, and H.-P. Nee

Published in *Proc. of* 16$^{\text{th}}$ *European Conference on Power Electronics and Applications (EPE 2014)*, 26–28 Aug. 2014.

©2014 EPE Association. Reprinted with permission.

Publication VI

An experimental analysis on how the dead-time of SiC BJT and SiC MOSFET impacts the losses in a high-frequency resonant converter

G. Tolstoy, P. Ranstad, Juan Colmenares, D. Peftitsis, F. Giezendanner, J. Rabkowski, and H.-P. Nee

Submitted for review.

©2015 IEEE. Reprinted with permission.

Publication VII

Dual control used in series-loaded resonant converter with SiC devices

G. Tolstoy, P. Ranstad, Juan Colmenares, F. Giezendanner, and H.-P. Nee

Accepted to be presented on *IEEE IPEC/ECCEASIA 2015*.

©2015 IEEE. Reprinted with permission.

Publication VIII

Experimental evaluation of SiC BJT and SiC MOSFET in a series resonant converter

G. Tolstoy, P. Ranstad, Juan Colmenares, F. Giezendanner, and H.-P. Nee

Accepted to be presented on *IEEE EPE 2015* Reprinted in this thesis is the abstract.

©2015 EPE Association. Reprinted with permission.